

On Predicting Mössbauer Parameters of Iron-containing Molecules with Density-Functional Theory

Mátyás Pápai,* György Vankó,

Wigner Research Centre for Physics, Hungarian Academy of Sciences, H-1525 Budapest,
P. O. Box 49., Hungary

Derivation of the electric monopole and quadrupole hyperfine interactions	p.S2
Derivation of the ligand contributions to V_{zz} for the octahedral FeA_2B_4 and FeAB_5 complexes	p.S5
Table S1 Contributions to the valence Fe-3d electrons to the V_{zz}	p.S6
Figure S1 The electronic configurations relevant to Fe(II), Fe(III) spin-crossover and to the inversion of the orbital ground state	p.S7
Table S2 Linear fit parameters obtained for the calculation of isomer shifts	p.S8
Table S3 Linear fit parameters obtained with the application of the COSMO model, for the calculation of isomer shifts	p.S9
Table S4 Comparison of experimental and DFT/GTO-CP(PPP) calculated δ values for the investigated data set of Fe complexes	p.S9
Table S5 Comparison of experimental and DFT/STO-TZP calculated δ values for the investigated data set of Fe complexes	p.S12
Table S6 Comparison of experimental and COSMO-DFT/GTO-CP(PPP) calculated δ values for the investigated data set of Fe complexes	p.S14
Table S7 Comparison of experimental and COSMO-DFT/STO-TZP calculated δ values for the investigated data set of Fe complexes	p.S17
Table S8 Comparison of experimental and DFT/GTO-CP(PPP) calculated ΔE_Q values for the investigated data set of Fe complexes	p.S19
Table S9 Comparison of experimental and DFT/STO-TZP calculated ΔE_Q values for the investigated data set of Fe complexes	p.S22
Table S10 Comparison of experimental and COSMO-DFT/GTO-CP(PPP) calculated ΔE_Q values for the investigated data set of Fe complexes	p.S24
Table S11 Comparison of experimental and COSMO-DFT/STO-TZP calculated ΔE_Q values for the investigated data set of Fe complexes	p.S27
Table S12 Comparison of experimental and COSMO-TPSSh $ \Delta E_Q $ values for selected Fe complexes computed with the GTO-CP(PPP) basis set at different geometries	p.S29
Table S13 DFT-calculated values of the asymmetry parameter (η) obtained with the GTO-CP(PPP) basis set	p.S30
Table S14 DFT-calculated values of the asymmetry parameter (η) obtained with the STO-TZP basis set	p.S32

Table S15 DFT-calculated ΔE_Q values obtained for the <i>cis-trans</i> isomers of FeA_4B_2 and for the FeA_5B low-spin, model compounds	p.S35
Table S16 Comparison of the experimental and DFT-calculated signs of V_{zz}	p.S35
Figure S2 Linear fit obtained for the electron density at the ^{57}Fe nucleus and experimental isomer shifts for the OLYP and B3LYP* methods in combination with the GTO-C(PPP) basis set	p.S38
Figure S3 Linear fit obtained for the electron density at the ^{57}Fe nucleus and experimental isomer shifts for the OLYP and B3LYP* methods in combination with the STO-TZP basis set	p.S39
Figure S4 Linear fit obtained for the electron density at the ^{57}Fe nucleus and experimental isomer shifts for the TPSS and TPSSh methods in combination with the GTO-C(PPP) basis set	p.S40
Figure S5 Linear fit obtained for the electron density at the ^{57}Fe nucleus and experimental isomer shifts for the TPSS and TPSSh methods in combination with the STO-TZP basis set	p.S41
Figure S6 Comparison of experimental and DFT-calculated quadrupole splittings obtained with the OLYP and B3LYP* methods in combination with the GTO-C(PPP) basis set	p.S42
Figure S7 Comparison of experimental and DFT-calculated quadrupole splittings obtained with the OLYP and B3LYP* methods in combination with the STO-TZP basis set	p.S43
Figure S8 Comparison of experimental and DFT-calculated quadrupole splittings obtained with the TPSS and TPSSh methods in combination with the GTO-C(PPP) basis set	p.S44
Figure S9 Comparison of experimental and DFT-calculated quadrupole splittings obtained with the TPSS and TPSSh methods in combination with the STO-TZP basis set	p.S45

Derivation of the electric monopole and quadrupole hyperfine interactions

In the present work we do not consider magnetic interactions here, as is beyond the scope of this study. We only deal with the electric hyperfine interactions, which is outlined below.

The substitution of the Taylor series expansion of the electric potential $\Phi(\mathbf{r})$ at the nucleus ($\mathbf{r} = 0$)

$$\Phi(\mathbf{r}) = \Phi(0) + \sum_{\alpha=1}^3 \left. \frac{\partial \Phi}{\partial x_{\alpha}} \right|_{\mathbf{r}=0} x_{\alpha} + \frac{1}{2} \sum_{\alpha, \beta=1}^3 \left. \frac{\partial^2 \Phi}{\partial x_{\alpha} \partial x_{\beta}} \right|_{\mathbf{r}=0} x_{\alpha} x_{\beta} + \dots \quad (\text{S1})$$

to the electric interaction energy E_{int} yields:

$$E_{\text{int}} = \int \rho_n(\mathbf{r}) \Phi(\mathbf{r}) d^3 \mathbf{r} = \Phi(0) \int \rho_n(\mathbf{r}) d^3 \mathbf{r} + \sum_{\alpha=1}^3 \left. \frac{\partial \Phi}{\partial x_{\alpha}} \right|_{\mathbf{r}=0} \int \rho_n(\mathbf{r}) x_{\alpha} d^3 \mathbf{r} + \frac{1}{2} \sum_{\alpha, \beta=1}^3 \left. \frac{\partial^2 \Phi}{\partial x_{\alpha} \partial x_{\beta}} \right|_{\mathbf{r}=0} \int \rho_n(\mathbf{r}) x_{\alpha} x_{\beta} d^3 \mathbf{r} + \dots \quad (\text{S2})$$

Since $\int \rho_n(\mathbf{r})d^3\mathbf{r} = Ze$, the nuclear charge, the interaction described by the first term of the right-hand side of Equation S2 shifts all nuclear levels by an equal amount: therefore, it does not affect the nuclear transitions. Furthermore, the second term vanishes, as the dipole moment of the nucleus is zero ($\int \rho_n(\mathbf{r})x_\alpha d^3\mathbf{r} = 0$).

Therefore, only the third term is relevant for the Mössbauer transition, and what is left from the potential is a tensor of its second derivatives. The first derivative of the electric potential is the electric field $\mathbf{E} = -\frac{\partial\Phi}{\partial x_\alpha}$; thus the negative second derivatives make up the electric field

gradient (EFG). Introducing the traceless electric field gradient (EFG) tensor:

$$V_{\alpha\beta}(\mathbf{r}) = -\left[\frac{\partial^2\Phi(\mathbf{r})}{\partial x_\alpha\partial x_\beta} - \frac{1}{3}\Delta\Phi(\mathbf{r})\delta_{\alpha\beta} \right] \quad (\text{S3})$$

the third term of Equation S2 can be further transformed as:

$$\begin{aligned} & \frac{1}{2} \sum_{\alpha,\beta=1}^3 \frac{\partial^2\Phi}{\partial x_\alpha\partial x_\beta} \Big|_{\mathbf{r}=0} \int \rho_n(\mathbf{r})x_\alpha x_\beta d^3\mathbf{r} = \\ & \frac{1}{2} \sum_{\alpha,\beta=1}^3 \left[-V_{\alpha\beta}(0) + \frac{1}{3}\Delta\Phi(0)\delta_{\alpha\beta} \right] \left[\int \rho_n(\mathbf{r}) \left(x_\alpha x_\beta - \frac{\mathbf{r}^2}{3} \delta_{\alpha\beta} \right) d^3\mathbf{r} + \int \rho_n(\mathbf{r}) \frac{\mathbf{r}^2}{3} \delta_{\alpha\beta} d^3\mathbf{r} \right] \end{aligned} \quad (\text{S4})$$

Since

$$\begin{aligned} & \sum_{\alpha,\beta=1}^3 \Delta\Phi(0)\delta_{\alpha\beta} \int \rho_n(\mathbf{r}) \left(x_\alpha x_\beta - \frac{\mathbf{r}^2}{3} \delta_{\alpha\beta} \right) d^3\mathbf{r} = \sum_{\alpha=1}^3 \Delta\Phi(0) \int \rho_n(\mathbf{r}) \left(x_\alpha^2 - \frac{\mathbf{r}^2}{3} \right) d^3\mathbf{r} = \\ & \int \Delta\Phi(0)\rho_n(\mathbf{r}) \left(x_1^2 - \frac{\mathbf{r}^2}{3} + x_2^2 - \frac{\mathbf{r}^2}{3} + x_3^2 - \frac{\mathbf{r}^2}{3} \right) d^3\mathbf{r} = 0 \end{aligned} \quad (\text{S5})$$

where $x_1^2 + x_2^2 + x_3^2 = \mathbf{r}^2$ and

$$\sum_{\alpha,\beta=1}^3 V_{\alpha\beta}(0) \int \rho_n(\mathbf{r}) \frac{\mathbf{r}^2}{3} \delta_{\alpha\beta} d^3\mathbf{r} = \sum_{\alpha=1}^3 V_{\alpha\alpha} \int \rho_n(\mathbf{r}) \frac{\mathbf{r}^2}{3} \delta_{\alpha\alpha} d^3\mathbf{r} = 0 \quad \left(\sum_{\alpha=1}^3 V_{\alpha\alpha} = 0 \right) \quad (\text{S6})$$

these two terms of Equation S4 vanish. Therefore, we have derived the expression given in Equation 2 of the main article:

$$E_{\text{int}}(2) = \frac{1}{6} \Delta\Phi(0) \int \rho_n(\mathbf{r}) \mathbf{r}^2 d^3\mathbf{r} - \frac{1}{2} \sum_{\alpha,\beta=1}^3 V_{\alpha\beta}(0) \int \rho_n(\mathbf{r}) \left(x_\alpha x_\beta - \frac{r^2}{3} \delta_{\alpha\beta} \right) d^3\mathbf{r} \quad (\text{S7})$$

The first, electric monopole term of Equation S7 can be written as:

$$E_M = \frac{1}{6} \Delta\Phi(0) \int \rho_n(\mathbf{r}) \mathbf{r}^2 d^3\mathbf{r} = \frac{1}{6} \Delta\Phi(0) Ze \langle r^2 \rangle = -\frac{1}{6\epsilon_0} \rho_e(0) Ze \langle r^2 \rangle = -\frac{Ze}{10\epsilon_0} \rho_e(0) R^2 \quad (\text{S8})$$

Here, $R = \sqrt{\frac{5}{3} \langle r^2 \rangle}$ is the radius of the nucleus, regarded as a sphere with a homogeneous charge density. Also, the first Maxwell-equation was applied:

$$\text{div } \mathbf{E}(\mathbf{r}) = \text{div}(-\text{grad } \Phi(\mathbf{r})) = -\Delta\Phi(\mathbf{r}) = \frac{\rho_e(\mathbf{r})}{\epsilon_0} \quad (\text{S9})$$

We can realize that this is the term where the trace of the original EFG tensor, $\Delta\Phi$, is utilized.

The second, electric quadrupole term shown in Equation S7 can be expressed as:

$$E_Q = -\frac{1}{2} \sum_{\alpha,\beta=1}^3 V_{\alpha\beta}(0) \int \rho_n(\mathbf{r}) \left(x_\alpha x_\beta - \frac{r^2}{3} \delta_{\alpha\beta} \right) d^3\mathbf{r} = -\frac{1}{2} \sum_{\alpha,\beta=1}^3 V_{\alpha\beta}(0) Q_{\alpha\beta} \quad (\text{S10})$$

from which Equation 7 of the main article is obtained by the diagonalization of the $V_{\alpha\beta}$ and $Q_{\alpha\beta}$ tensors. Since the diagonalized EFG tensor

$$V_{\alpha\alpha} = - \begin{pmatrix} V_{xx} & 0 & 0 \\ 0 & V_{yy} & 0 \\ 0 & 0 & V_{zz} \end{pmatrix} \quad (\text{S11})$$

is traceless, it can be characterized by two independent parameters: the main tensor component V_{zz} , and the asymmetry parameter $\eta = (V_{xx} - V_{yy}) / V_{zz}$ (with $|V_{zz}| \geq |V_{yy}| \geq |V_{xx}|$).

The negative sign is due to the convention used in the Mössbauer literature, which considers the EFG as the second derivative of the potential, without the correct sign). We also adapt to this convention, and the quantities defined this way have letters of the Latin alphabet for

indices (V_{xx} , V_{yy} , V_{zz}) in contrast to the physically correct ones indicated by Greek letters in the indices.

Derivation of the ligand contributions to the V_{zz} for the octahedral FeA_2B_4 and FeAB_5 complexes

Considering a potential $\Phi = q/r$ generated by a point charge q , the components of the diagonalized and traceless EFG are expressed as:

$$V_{xx} = \frac{\partial^2 \Phi}{\partial x^2} = q(3x^2 - r^2)r^{-5} = q(3 \sin^2 \vartheta \cos^2 \varphi - 1)r^{-3} \quad (\text{S12a})$$

$$V_{yy} = \frac{\partial^2 \Phi}{\partial y^2} = q(3y^2 - r^2)r^{-5} = q(3 \sin^2 \vartheta \sin^2 \varphi - 1)r^{-3} \quad (\text{S12b})$$

$$V_{zz} = \frac{\partial^2 \Phi}{\partial z^2} = q(3z^2 - r^2)r^{-5} = q(3 \cos^2 \vartheta - 1)r^{-3} \quad (\text{S12c})$$

Here the x , y , and z coordinates were transformed to polar coordinates (ϑ is the angle between the z axis and the position vector of the q charge, φ is the angle in the xy plane.). Selecting the proper orientation for x , y , and z , and if the charge distribution is similar in the x and y directions, it is sufficient to deal with the V_{zz} .

In case of a low-spin, octahedral $\text{trans-Fe}^{\text{II}}\text{A}_2\text{B}_4$ complex (where A and B are point charges, see Figure 8 in the main article), for the two q_{A} charges:

$$V_{zz} = 2q_{\text{A}}(3 \cos^2(0^\circ) - 1) = 4q_{\text{A}} \quad (\text{S13})$$

and for the four q_{B} charges:

$$V_{zz} = 4q_{\text{B}}(3 \cos^2(90^\circ) - 1) = -4q_{\text{B}} \quad (\text{S14})$$

Therefore, the total V_{zz} equals $4(q_{\text{A}} - q_{\text{B}})$. Similarly, the $-2(q_{\text{A}} - q_{\text{B}})$ and $2(q_{\text{A}} - q_{\text{B}})$ values are derived for the $\text{cis-Fe}^{\text{II}}\text{A}_2\text{B}_4$ and $\text{Fe}^{\text{II}}\text{AB}_5$ complexes, respectively. Note that in all these cases, $\eta = 0$, due to the axial symmetry and that no unpaired electron contributes to the EFG, since

these systems possess a closed d^6 sub-shell. Thus, the 2: -1 : 1 ratio of the quadrupole splittings of the *trans*- $\text{Fe}^{\text{II}}\text{A}_2\text{B}_4$, *cis*- $\text{Fe}^{\text{II}}\text{A}_2\text{B}_4$ and $\text{Fe}^{\text{II}}\text{AB}_5$ complexes is derived.

Contributions of the valence Fe-3d electrons to V_{zz}

In addition to the ligand contributions, a non-zero V_{zz} can also arise due to the asymmetric occupation of the valence Fe-3d orbitals. The contribution of an arbitrary valence electron can be evaluated by calculating the

$$(V_{zz})_{\text{val}} = \langle \psi_i | 3\cos^2 \vartheta - 1 | \psi_i \rangle \langle r_i^{-3} \rangle \quad (\text{S15})$$

expectation value (ψ_i is the molecular orbital occupied by the valence electron). Substituting ψ_i with the five Fe-3d orbitals, the following values are obtained for the electron-only contributions to the V_{zz} :

Table S1. Contributions of the valence 3d-electrons to the V_{zz}

orbital	$(V_{zz})_{\text{val}} / e \langle r^{-3} \rangle$
d_{xy}	+4/7
d_{xz}	-2/7
d_{yz}	-2/7
$d_{x^2-y^2}$	+4/7
d_{z^2}	-4/7

In the frequent tetrahedral and octahedral coordinations the symmetry splits the five Fe-3d orbitals into a threefold degenerate t_{2g} , and a twofold degenerate e_g sub-shells, which include the d_{xy} , d_{xz} , and d_{yz} , and the $d_{x^2-y^2}$, d_{z^2} orbitals, respectively.

Using the above table an important observation can be made: the evenly filled t_{2g} and e_g sub-shells do not contribute to the EFG. This includes all the following configurations and their possible combinations: $(t_{2g})^0$, $(t_{2g})^3$, $(t_{2g})^6$, $(e_g)^0$, $(e_g)^2$, $(e_g)^4$ (see Figure S1, below).

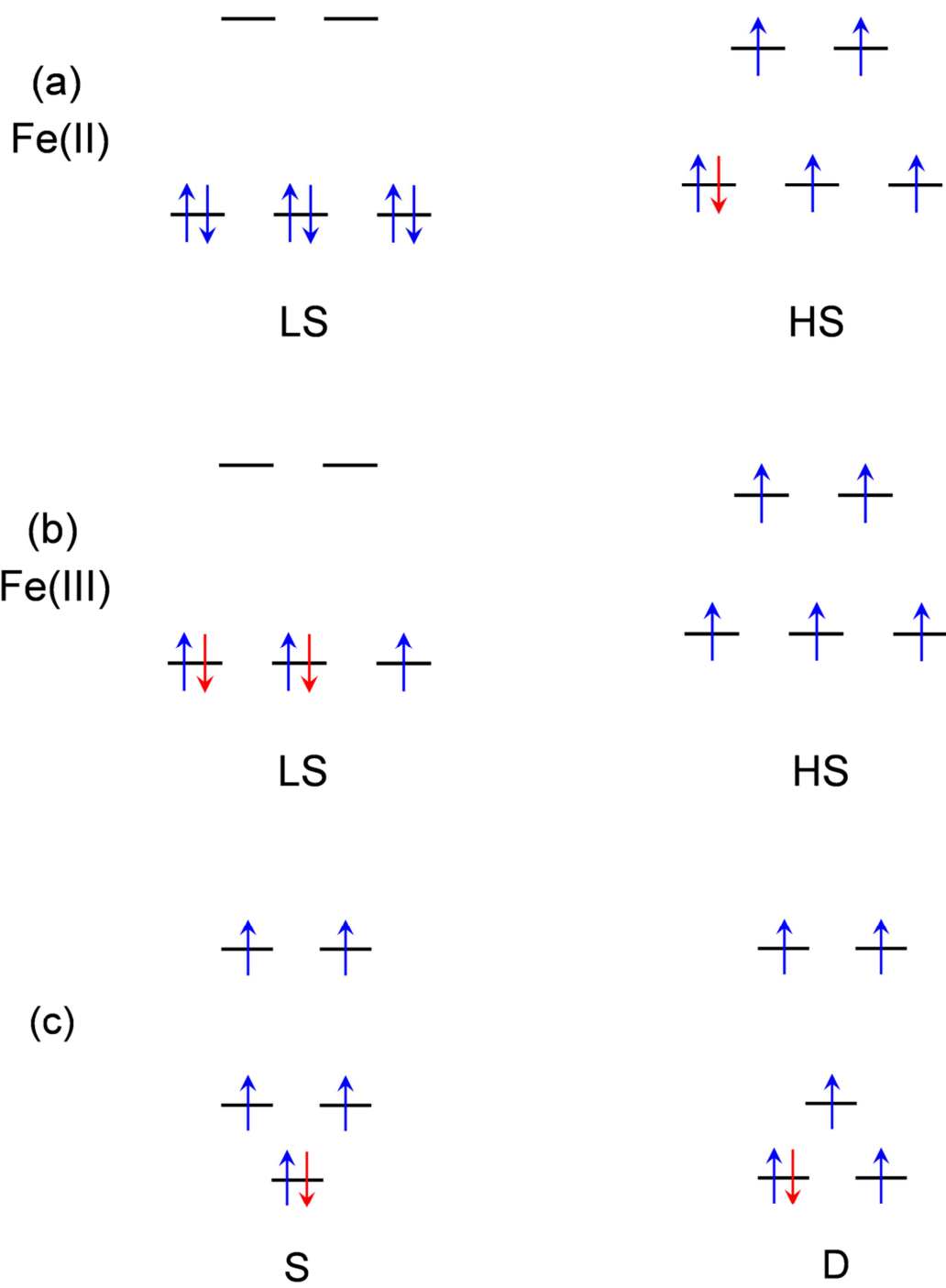


Figure S1. The low-spin (LS), high-spin (HS), orbital singlet (S), doublet (D) electronic configurations relevant to (a) Fe(II), (b) Fe(III) spin-crossover and to (c) the inversion of the orbital ground state. The electrons contributing to the EFG are indicated in red.

Table S2. Linear fit parameters obtained for the $\delta = \alpha(\rho(0) - c) + \beta$ calculation of isomer shifts

method	α (au ³ mms ⁻¹)	β (mms ⁻¹)
GTO-CP(PPP) basis		
RPBE	-0.458 ± 0.017	12.86 ± 0.46
OLYP	-0.466 ± 0.019	4.55 ± 0.17
B3LYP	-0.431 ± 0.009	7.66 ± 0.15
B3LYP*	-0.439 ± 0.011	6.75 ± 0.15
TPSS	-0.463 ± 0.015	10.33 ± 0.32
TPSSh	-0.443 ± 0.011	9.38 ± 0.22
STO-TZP basis		
RPBE	-0.464 ± 0.018	16.36 ± 0.63
OLYP	-0.367 ± 0.020	7.97 ± 0.41
B3LYP	-0.419 ± 0.008	10.40 ± 0.20
B3LYP*	-0.433 ± 0.010	9.34 ± 0.21
TPSS	-0.485 ± 0.016	17.79 ± 0.59
TPSSh	-0.452 ± 0.012	16.28 ± 0.44

Table S3. Linear fit parameters obtained with the application of the COSMO model for the $\delta = \alpha(\rho(0) - c) + \beta$ calculation of isomer shifts

method	α (au ³ mms ⁻¹)	β (mms ⁻¹)
GTO-CP(PPP) basis		
RPBE	-0.459 ± 0.014	12.91 ± 0.38
OLYP	-0.448 ± 0.014	4.40 ± 0.13
B3LYP	-0.424 ± 0.007	7.55 ± 0.12
B3LYP*	-0.439 ± 0.008	6.77 ± 0.12
TPSS	-0.462 ± 0.012	10.33 ± 0.26
TPSSh	-0.442 ± 0.008	9.39 ± 0.17
STO-TZP basis		
RPBE	-0.474 ± 0.015	16.73 ± 0.52
OLYP	-0.371 ± 0.017	8.06 ± 0.35
B3LYP	-0.422 ± 0.007	10.47 ± 0.16
B3LYP*	-0.436 ± 0.008	9.42 ± 0.17
TPSS	-0.498 ± 0.015	18.25 ± 0.54
TPSSh	-0.459 ± 0.011	16.54 ± 0.38

Table S4. Comparison of experimental and DFT/GTO-CP(PPP) calculated δ values for the investigated data set of Fe complexes (values are given in mms⁻¹)

complex	exptl. ^a	RPBE	OLYP	B3LYP	B3LYP*	TPSS	TPSSh
1	0.37	0.29	0.29	0.42	0.38	0.31	0.35
2	0.47	0.32	0.32	0.43	0.40	0.34	0.37
3	0.46	0.52	0.52	0.60	0.58	0.53	0.55
4	0.27	0.19	0.19	0.24	0.22	0.21	0.21
5	-0.15	-0.21	-0.05	-0.18	-0.19	-0.20	-0.20
6	0.02	-0.04	-0.06	-0.01	-0.02	-0.02	-0.03
7	0.03	-0.02	-0.04	0.00	0.00	-0.01	-0.02

8	0.56	0.65	0.65	0.70	0.70	0.66	0.65
9	0.08	0.10	0.08	0.18	0.16	0.12	0.13
10	0.27	0.31	0.31	0.23	0.37	0.34	0.34
11	0.28	0.17	0.15	0.24	0.22	0.19	0.20
12	0.11	0.04	0.03	0.11	0.10	0.06	0.07
13	0.06	-0.01	-0.04	0.06	0.05	0.02	0.03
14	0.05	-0.05	-0.07	0.03	0.01	-0.02	-0.01
15	-0.12	-0.20	-0.22	-0.10	-0.21	-0.17	-0.14
16	-0.14	-0.28	-0.30	-0.19	-0.21	-0.25	-0.23
17	0.36	0.31	0.31	0.43	0.39	0.33	0.36
18	0.37	0.34	0.34	0.46	0.43	0.36	0.40
19	0.30	0.21	0.21	0.33	0.30	0.23	0.26
20	1.04	0.84	0.86	0.96	0.91	0.87	0.90
21	1.13	0.85	0.87	0.98	0.93	0.88	0.92
22	1.09	1.07	1.11	1.11	1.09	1.09	1.09
23	0.67	0.62	0.67	0.61	0.61	0.64	0.62
24	0.66	0.61	0.64	0.62	0.61	0.64	0.62
25	1.10	0.83	0.85	0.95	0.90	0.86	0.89
26	1.10	0.97	1.00	1.06	1.11	1.01	1.12
27	1.05	0.84	0.85	1.02	0.97	0.87	0.95
28	1.03	0.81	0.82	0.99	0.94	0.84	0.91
29	1.11	0.87	0.89	0.99	0.95	0.90	0.93
30	1.19	0.96	0.98	1.07	1.04	1.00	1.03
31	1.38	1.41	1.46	1.42	1.42	1.42	1.41
32	1.00	1.12	0.72	1.10	1.11	1.13	1.11
33	0.97	1.06	0.70	1.03	1.05	1.08	1.05
34	0.62	0.55	0.62	0.55	0.52	0.59	0.60
35	0.52	0.57	0.61	0.54	0.51	0.59	0.61
36	0.31	0.22	0.23	0.22	0.23	0.23	0.20

37	0.28	0.23	0.38	0.22	0.22	0.22	0.20
38	0.09	0.18	0.18	0.18	0.18	0.18	0.16
39	0.13	0.22	0.22	0.21	0.21	0.21	0.20
40	0.08	0.11	0.11	0.12	0.12	0.11	0.10
41	0.31	0.39	0.40	0.34	0.35	0.38	0.34
42	0.26	0.32	0.32	0.29	0.29	0.31	0.28
43	0.57	0.61	0.64	0.53	0.55	0.61	0.54
44	0.46	0.63	0.65	0.54	0.56	0.61	0.55
45	0.25	0.27	0.29	0.19	0.20	0.28	0.22
46	0.43	0.53	0.56	0.45	0.47	0.52	0.46
47	0.60	0.76	0.78	0.66	0.68	0.74	0.67
48	0.56	0.75	0.79	0.65	0.67	0.72	0.65
49	0.56	0.75	0.78	0.65	0.67	0.73	0.66
50	0.53	0.78	0.81	0.65	0.68	0.75	0.67
51	0.33	0.48	0.50	0.38	0.40	0.47	0.40
52	0.39	0.49	0.52	0.39	0.41	0.49	0.42
53	0.56	0.77	0.81	0.65	0.67	0.76	0.68
54	0.69	0.80	0.83	0.71	0.73	0.77	0.71
55	0.50	0.49	0.51	0.46	0.46	0.50	0.46
56	0.25	0.32	0.34	0.27	0.28	0.31	0.27
57	0.39	0.30	0.31	0.31	0.29	0.32	0.29
58	0.17	0.25	0.26	0.20	0.20	0.23	0.19
59	-0.04	-0.01	-0.02	-0.02	-0.02	-0.02	-0.04
60	-0.04	0.09	0.10	-0.01	0.01	0.07	0.01
61	0.16	0.23	0.23	0.18	0.20	0.25	0.20
62	0.12	0.15	0.15	0.12	0.13	0.17	0.13

^a Experimental δ value corrected to 4.2K.

Table S5. Comparison of experimental and DFT/STO-TZP calculated δ values for the investigated data set of Fe complexes (values are given in mms^{-1})

complex	exptl. ^a	RPBE	OLYP	B3LYP	B3LYP*	TPSS	TPSSh
1	0.37	0.24	0.20	0.43	0.39	0.39	0.44
2	0.47	0.27	0.20	0.43	0.40	0.42	0.46
3	0.46	0.39	0.43	0.56	0.54	0.46	0.53
4	0.27	0.28	0.19	0.27	0.25	0.29	0.29
5	-0.15	-0.19	-0.14	-0.22	-0.23	-0.24	-0.23
6	0.02	-0.01	-0.08	-0.03	-0.04	0.04	0.02
7	0.03	-0.06	-0.11	-0.02	-0.03	0.07	0.05
8	0.56	0.54	0.57	0.60	0.60	0.51	0.52
9	0.08	0.08	-0.01	0.15	0.14	0.21	0.20
10	0.27	0.34	0.19	0.37	0.36	0.45	0.43
11	0.28	-0.06	-0.11	-0.02	-0.03	0.07	0.05
12	0.11	0.06	-0.03	0.09	0.07	0.12	0.12
13	0.06	-0.02	-0.10	0.03	0.02	0.08	0.08
14	0.05	-0.04	-0.12	0.01	0.00	0.05	0.05
15	-0.12	-0.20	-0.24	-0.11	-0.14	-0.09	-0.07
16	-0.14	-0.30	-0.15	-0.22	-0.24	-0.31	-0.27
17	0.36	0.23	0.29	0.41	0.38	0.32	0.38
18	0.37	0.26	0.31	0.43	0.40	0.34	0.40
19	0.30	0.35	0.29	0.36	0.46	0.48	0.52
20	1.04	0.80	0.75	0.99	0.96	0.91	0.95
21	1.13	0.80	0.75	0.96	0.92	0.90	0.94
22	1.09	1.05	1.07	1.09	1.08	1.00	1.05
23	0.67	0.68	0.78	0.63	0.63	0.58	0.58
24	0.66	0.65	0.74	0.63	0.62	0.58	0.58
25	1.10	0.87	0.91	0.95	0.91	0.80	0.85
26	1.10	1.03	1.04	1.07	1.06	1.01	1.04

27	1.05	0.88	0.72	1.06	1.02	1.03	1.09
28	1.03	0.86	0.71	1.04	0.99	1.02	1.07
29	1.11	0.83	0.78	1.01	0.99	0.93	0.97
30	1.19	0.89	0.82	1.03	1.02	1.03	1.07
31	1.38	1.40	1.31	1.36	1.36	1.38	1.37
32	1.00	1.13	1.13	1.06	1.06	1.04	1.03
33	0.97	1.11	1.11	1.01	1.01	1.00	0.99
34	0.62	0.54	0.56	0.60	0.59	0.59	0.62
35	0.52	0.53	0.55	0.62	0.61	0.59	0.62
36	0.31	0.24	0.17	0.26	0.26	0.36	0.33
37	0.28	0.22	0.17	0.25	0.25	0.34	0.32
38	0.09	0.11	0.21	0.17	0.16	0.15	0.16
39	0.13	0.14	0.24	0.19	0.19	0.17	0.22
40	0.08	0.11	0.08	0.16	0.16	0.23	0.22
41	0.31	0.32	0.28	0.32	0.33	0.44	0.40
42	0.26	0.23	0.32	0.26	0.26	0.25	0.26
43	0.57	0.61	0.58	0.55	0.57	0.68	0.61
44	0.46	0.59	0.57	0.55	0.58	0.68	0.62
45	0.25	0.31	0.46	0.21	0.23	0.22	0.18
46	0.43	0.52	0.52	0.46	0.48	0.56	0.50
47	0.60	0.73	0.71	0.65	0.67	0.77	0.69
48	0.56	0.73	0.73	0.65	0.68	0.73	0.67
49	0.56	0.73	0.72	0.65	0.68	0.75	0.68
50	0.53	0.76	0.77	0.62	0.65	0.71	0.64
51	0.33	0.47	0.58	0.38	0.40	0.40	0.35
52	0.39	0.53	0.65	0.40	0.42	0.41	0.36
53	0.56	0.89	0.93	0.69	0.72	0.75	0.68
54	0.69	0.80	0.80	0.70	0.72	0.75	0.69
55	0.50	0.48	0.58	0.45	0.45	0.42	0.41

56	0.25	0.24	0.28	0.24	0.25	0.34	0.31
57	0.39	0.31	0.45	0.30	0.29	0.21	0.21
58	0.17	0.27	0.25	0.18	0.18	0.22	0.21
59	-0.04	0.06	0.07	0.00	-0.01	0.00	0.00
60	-0.04	0.06	0.08	0.00	0.02	0.16	0.09
61	0.16	0.14	0.30	0.14	0.15	0.11	0.11
62	0.12	0.10	0.29	0.08	0.08	-0.03	-0.01
63	-0.42	-0.35	-0.20	-0.47	-0.46	-0.48	-0.50
64	-0.02	0.03	0.10	-0.05	-0.05	-0.07	-0.07
65	-0.29	-0.30	-0.13	-0.33	-0.33	-0.34	-0.34
66	-0.82	-0.67	-0.55	-0.82	-0.81	-0.80	-0.84

^a Experimental δ value corrected to 4.2K.

Table S6. Comparison of experimental and COSMO-DFT/GTO-CP(PPP) calculated δ values for the investigated data set of Fe complexes (values are given in mms^{-1})

complex	exptl. ^a	RPBE	OLYP	B3LYP	B3LYP*	TPSS	TPSSh
1	0.37	0.36	0.36	0.47	0.45	0.39	0.42
2	0.47	0.39	0.39	0.48	0.46	0.41	0.44
3	0.46	0.53	0.52	0.59	0.58	0.55	0.57
4	0.27	0.19	0.19	0.23	0.22	0.21	0.22
5	-0.15	-0.19	-0.19	-0.15	-0.16	-0.17	-0.16
6	0.02	-0.01	-0.02	0.03	0.02	0.01	0.02
7	0.03	0.00	-0.01	0.03	0.03	0.03	0.02
8	0.56	0.67	0.66	0.70	0.71	0.69	0.68
9	0.08	0.00	-0.01	0.08	0.06	0.03	0.04
10	0.27	0.18	0.17	0.24	0.23	0.21	0.22
11	0.28	0.19	0.18	0.25	0.24	0.22	0.22
12	0.11	0.04	0.04	0.10	0.09	0.07	0.08

13	0.06	-0.03	-0.03	0.05	0.03	0.01	0.02
14	0.05	-0.05	-0.05	0.02	0.01	-0.01	0.00
15	-0.12	-0.19	-0.19	-0.10	-0.12	-0.15	-0.13
16	-0.14	-0.27	-0.27	-0.18	-0.20	-0.23	-0.21
17	0.36	0.31	0.31	0.41	0.39	0.34	0.37
18	0.37	0.35	0.35	0.45	0.43	0.38	0.41
19	0.30	0.21	0.21	0.32	0.30	0.24	0.28
<hr/>							
20	1.04	0.94	0.94	1.03	1.02	0.98	1.01
21	1.13	0.92	0.91	1.04	0.99	0.95	0.98
22	1.09	1.08	1.08	1.10	1.10	1.10	1.11
23	0.67	0.64	0.66	0.62	0.62	0.66	0.65
24	0.66	0.61	0.63	0.60	0.60	0.64	0.63
25	1.10	0.91	0.91	1.01	1.00	0.95	1.00
26	1.10	1.00	1.00	1.05	1.04	1.03	1.06
27	1.05	0.86	0.85	0.99	0.98	0.90	0.97
28	1.03	0.85	0.84	0.99	0.98	0.89	0.98
29	1.11	0.96	0.95	1.04	1.02	0.99	1.02
30	1.19	1.05	1.05	1.13	1.12	1.08	1.06
31	1.38	1.36	1.35	1.34	1.35	1.36	1.36
32	1.00	1.07	1.08	1.03	1.04	1.08	1.06
33	0.97	1.00	1.01	1.03	0.97	1.02	1.00
<hr/>							
34	0.62	0.51	0.60	0.53	0.52	0.50	0.53
35	0.52	0.60	0.62	0.65	0.64	0.62	0.65
<hr/>							
36	0.31	0.24	0.25	0.23	0.24	0.25	0.23
37	0.28	0.25	0.25	0.22	0.23	0.24	0.22
38	0.09	0.16	0.16	0.15	0.16	0.16	0.15
39	0.13	0.20	0.20	0.18	0.19	0.19	0.18
40	0.08	0.10	0.10	0.11	0.11	0.10	0.09
41	0.31	0.40	0.40	0.34	0.36	0.39	0.35

42	0.26	0.34	0.32	0.28	0.29	0.32	0.29
43	0.57	0.63	0.64	0.53	0.56	0.63	0.57
44	0.46	0.63	0.64	0.53	0.56	0.62	0.56
45	0.25	0.29	0.30	0.19	0.21	0.29	0.24
46	0.43	0.57	0.58	0.47	0.50	0.56	0.51
47	0.60	0.75	0.75	0.64	0.67	0.73	0.67
48	0.56	0.76	0.76	0.64	0.67	0.74	0.67
49	0.56	0.77	0.77	0.65	0.68	0.75	0.68
50	0.53	0.70	0.71	0.58	0.61	0.67	0.60
51	0.33	0.48	0.50	0.37	0.40	0.47	0.41
52	0.39	0.49	0.50	0.38	0.40	0.49	0.42
53	0.56	0.66	0.67	0.55	0.57	0.66	0.59
54	0.69	0.73	0.73	0.64	0.66	0.70	0.65
55	0.50	0.50	0.52	0.45	0.47	0.51	0.48
56	0.25	0.33	0.34	0.27	0.28	0.32	0.29
57	0.39	0.38	0.39	0.34	0.36	0.40	0.37
58	0.17	0.24	0.25	0.18	0.19	0.22	0.19
59	-0.04	-0.01	0.00	-0.03	-0.03	-0.01	-0.03
60	-0.04	0.10	0.12	0.00	0.02	0.09	0.03
61	0.16	0.25	0.25	0.19	0.21	0.28	0.23
62	0.12	0.15	0.16	0.12	0.13	0.18	0.14
63	-0.42	-0.39	-0.38	-0.46	-0.45	-0.40	-0.44
64	-0.02	-0.03	-0.02	-0.04	-0.05	-0.04	-0.05
65	-0.29	-0.29	-0.27	-0.34	-0.34	-0.31	-0.33
66	-0.82	-0.81	-0.79	-0.89	-0.89	-0.84	-0.88

^a Experimental δ value corrected to 4.2K.

Table S7. Comparison of experimental and COSMO-DFT/STO-TZP calculated δ values for the investigated data set of Fe complexes (values are given in mms^{-1})

complex	exptl. ^a	RPBE	OLYP	B3LYP	B3LYP*	TPSS	TPSSh
1	0.37	0.31	0.25	0.48	0.46	0.44	0.51
2	0.47	0.33	0.25	0.48	0.47	0.46	0.52
3	0.46	0.40	0.43	0.56	0.55	0.46	0.54
4	0.27	0.29	0.19	0.25	0.25	0.25	0.28
5	-0.15	-0.16	-0.14	-0.18	-0.18	-0.22	-0.19
6	0.02	0.01	-0.08	0.02	0.02	0.06	0.08
7	0.03	-0.05	-0.09	0.00	0.01	0.07	0.08
8	0.56	0.57	0.59	0.61	0.63	0.52	0.54
9	0.08	-0.01	-0.10	0.05	0.05	0.07	0.09
10	0.27	0.23	0.09	0.23	0.24	0.27	0.28
11	0.28	0.23	0.09	0.23	0.24	0.27	0.29
12	0.11	0.06	-0.04	0.07	0.07	0.08	0.10
13	0.06	-0.04	-0.12	0.00	0.00	0.03	0.05
14	0.05	-0.04	-0.12	0.00	0.00	0.02	0.04
15	-0.12	-0.20	-0.25	-0.13	-0.13	-0.12	-0.08
16	-0.14	-0.31	-0.16	-0.23	-0.24	-0.35	-0.28
17	0.36	0.23	0.28	0.39	0.38	0.30	0.38
18	0.37	0.27	0.31	0.43	0.41	0.33	0.41
19	0.30	0.22	0.14	0.36	0.34	0.34	0.40
20	1.04	0.92	0.88	1.04	1.01	0.94	1.01
21	1.13	0.89	0.88	1.01	0.98	0.88	0.96
22	1.09	1.08	1.07	1.09	1.10	1.00	1.06
23	0.67	0.70	0.78	0.64	0.65	0.57	0.59
24	0.66	0.65	0.74	0.62	0.63	0.56	0.58
25	1.10	0.98	0.98	1.02	1.02	0.90	0.97
26	1.10	1.05	1.04	1.08	1.08	1.02	1.07

27	1.05	0.87	0.80	1.00	1.00	0.94	1.02
28	1.03	0.86	0.75	1.01	1.02	0.99	1.08
29	1.11	0.93	0.90	1.02	1.01	0.94	1.01
30	1.19	0.99	0.94	1.09	1.09	0.99	1.09
31	1.38	1.37	1.27	1.31	1.33	1.32	1.32
32	1.00	1.08	1.07	1.00	1.02	0.97	0.98
33	0.97	1.05	1.05	0.94	0.96	0.92	0.92
34	0.62	0.57	0.57	0.61	0.62	0.60	0.65
35	0.52	0.57	0.57	0.64	0.64	0.60	0.65
36	0.31	0.26	0.19	0.27	0.28	0.35	0.34
37	0.28	0.23	0.17	0.24	0.26	0.32	0.32
38	0.09	0.08	0.17	0.14	0.15	0.11	0.15
39	0.13	0.11	0.20	0.16	0.17	0.13	0.17
40	0.08	0.10	0.06	0.14	0.15	0.19	0.21
41	0.31	0.33	0.28	0.32	0.34	0.42	0.40
42	0.26	0.25	0.33	0.26	0.28	0.24	0.27
43	0.57	0.64	0.62	0.56	0.59	0.66	0.61
44	0.46	0.61	0.58	0.54	0.58	0.65	0.61
45	0.25	0.31	0.46	0.20	0.24	0.19	0.18
46	0.43	0.56	0.55	0.48	0.52	0.58	0.54
47	0.60	0.74	0.70	0.65	0.69	0.76	0.71
48	0.56	0.76	0.74	0.65	0.69	0.73	0.68
49	0.56	0.76	0.74	0.66	0.70	0.75	0.70
50	0.53	0.68	0.66	0.56	0.60	0.66	0.60
51	0.33	0.48	0.58	0.37	0.41	0.38	0.35
52	0.39	0.53	0.64	0.38	0.42	0.38	0.35
53	0.56	0.77	0.82	0.60	0.64	0.61	0.58
54	0.69	0.71	0.66	0.63	0.67	0.70	0.67
55	0.50	0.51	0.62	0.45	0.47	0.40	0.40

56	0.25	0.30	0.27	0.27	0.29	0.38	0.36
57	0.39	0.41	0.53	0.33	0.36	0.25	0.26
58	0.17	0.25	0.23	0.15	0.17	0.18	0.19
59	-0.04	0.06	0.06	-0.02	0.00	-0.02	0.00
60	-0.04	0.07	0.08	0.00	0.03	0.14	0.10
61	0.16	0.16	0.32	0.14	0.17	0.10	0.12
62	0.12	0.11	0.29	0.07	0.09	-0.05	-0.02
63	-0.42	-0.34	-0.20	-0.47	-0.45	-0.50	-0.50
64	-0.02	-0.01	0.08	-0.09	-0.07	-0.14	-0.11
65	-0.29	-0.33	-0.16	-0.37	-0.35	-0.41	-0.37
66	-0.82	-0.67	-0.56	-0.83	-0.80	-0.84	-0.84

^a Experimental δ value corrected to 4.2K.

Table S8. Comparison of experimental and DFT/GTO-CP(PPP) calculated $|\Delta E_Q|$ values for the investigated data set of Fe complexes (values are given in mms^{-1})

complex	exptl.	RPBE	OLYP	B3LYP	B3LYP*	TPSS	TPSSh
1	0.34	0.69	0.68	0.44	0.52	0.65	0.55
2	0.77	1.18	1.17	0.77	0.88	1.07	0.89
3	0.21	0.04	0.04	0.10	0.07	0.03	0.09
4	1.84	1.76	1.76	1.59	1.63	1.69	1.63
5	1.72	1.95	1.99	2.18	2.14	1.95	2.07
6	2.75	2.93	2.95	3.16	3.12	2.92	3.03
7	2.86	2.53	2.55	3.39	3.13	2.59	2.94
8	2.38	2.44	2.44	3.27	3.07	2.50	2.85
9	1.88	1.83	1.83	2.06	2.02	1.84	1.94
10	1.82	1.76	1.75	2.06	2.00	1.78	1.91
11	1.87	1.69	1.69	1.98	1.92	1.72	1.84
12	1.76	1.74	1.74	2.07	2.00	1.76	1.90
13	1.46	1.44	1.45	1.58	1.55	1.45	1.50

14	1.52	1.58	1.58	1.70	1.68	1.58	1.63
15	2.52	2.10	2.17	2.45	2.37	2.15	2.30
16	1.36	1.13	1.16	1.27	1.23	1.15	1.21
17	0.39	0.49	0.48	0.31	0.36	0.43	0.35
18	0.25	0.42	0.42	0.26	0.31	0.38	0.31
19	1.00	0.94	0.95	0.93	0.94	0.92	0.90
20	2.82	1.92	1.85	3.09	2.80	2.12	2.70
21	2.51	1.77	1.74	2.39	2.27	1.88	2.20
22	3.86	3.66	3.69	3.85	3.81	3.66	3.76
23	4.01	3.69	3.64	4.14	4.06	3.73	4.00
24	3.24	2.67	2.73	3.22	3.09	2.70	3.01
25	3.27	2.00	1.92	3.13	2.83	2.20	2.73
26	3.14	2.62	2.55	3.28	3.11	2.78	3.09
27	4.25	2.56	2.36	4.13	3.87	2.83	3.63
28	4.01	2.40	2.20	3.97	3.63	2.64	3.41
29	3.27	2.10	2.03	3.19	2.95	2.29	2.85
30	2.14	1.89	1.87	2.26	2.21	1.99	2.18
31	3.38	3.28	3.30	3.42	3.40	3.28	3.33
32	3.30	3.63	3.62	3.80	3.80	3.63	3.71
33	3.23	3.58	3.58	3.79	3.78	3.59	3.69
34	1.60	1.47	1.92	0.31	0.40	1.35	1.09
35	1.51	1.75	2.01	0.34	0.43	1.46	1.20
36	3.09	2.88	2.87	3.47	3.36	2.91	3.20
37	2.24	2.01	2.03	2.24	2.20	1.93	2.06
38	1.90	2.04	2.08	2.05	2.07	1.92	1.92
39	1.84	2.10	2.14	2.12	2.14	1.96	2.38
40	3.43	3.73	3.74	4.27	4.17	3.59	4.01
41	2.24	1.79	1.82	1.82	1.89	1.67	1.72
42	2.15	2.31	2.35	2.38	2.39	2.13	2.14

43	0.81	1.07	1.08	1.18	1.16	1.06	1.12
44	0.53	0.76	0.75	0.71	0.73	0.75	0.72
45	0.62	0.63	0.63	0.52	0.56	0.58	0.51
46	0.98	0.71	0.71	0.69	0.70	0.71	0.71
47	0.76	0.67	0.67	0.77	0.73	0.67	0.73
48	0.64	0.77	0.76	0.67	0.70	0.75	0.70
49	0.67	0.80	0.79	0.72	0.75	0.78	0.74
50	0.00	0.00	0.00	0.00	0.00	0.00	0.01
51	0.00	0.01	0.01	0.00	0.00	0.01	0.01
52	0.00	0.00	0.00	0.00	0.00	0.00	0.00
53	0.00	0.00	0.00	0.00	0.00	0.00	0.00
54	0.00	0.03	0.03	0.03	0.03	0.03	0.03
<hr/>							
55	2.70	1.83	1.91	2.22	2.12	1.78	2.01
56	3.60	3.04	3.12	3.34	3.27	2.97	3.17
57	2.64	2.21	2.37	2.94	2.73	2.12	2.54
<hr/>							
58	1.24	1.00	1.00	0.98	0.99	0.99	0.99
59	0.93	0.50	0.50	0.86	0.80	0.53	0.70
60	0.89	0.85	0.89	0.91	0.90	0.83	0.87
61	1.52	1.79	1.83	2.30	2.15	1.77	2.03
62	3.03	2.90	2.94	3.32	3.22	2.89	3.08
<hr/>							
63	4.25	3.86	3.88	4.22	4.13	3.75	3.95
64	1.60	1.63	1.66	1.89	1.77	1.59	1.70
<hr/>							
65	1.53	0.72	0.77	0.76	0.76	0.67	0.71
66	0.00	0.01	0.01	0.01	0.01	0.01	0.01

Table S9. Comparison of experimental and DFT/STO-TZP calculated $|\Delta E_Q|$ values for the investigated data set of Fe complexes (values are given in mms^{-1})

complex	exptl.	RPBE	OLYP	B3LYP	B3LYP*	TPSS	TPSSh
1	0.34	0.64	0.63	0.40	0.48	0.61	0.51
2	0.77	1.17	1.14	0.80	0.90	1.05	0.89
3	0.21	0.02	0.03	0.15	0.12	0.07	0.13
4	1.84	1.80	1.79	1.60	1.64	1.71	1.63
5	1.72	1.95	1.99	2.17	2.12	1.93	2.05
6	2.75	2.85	2.87	3.09	3.05	2.83	2.95
7	2.86	2.50	2.51	3.36	3.11	2.57	2.92
8	2.38	2.46	2.50	3.39	3.18	2.53	2.98
9	1.88	1.70	1.71	1.92	1.88	1.72	1.82
10	1.82	1.63	1.63	1.92	1.86	1.65	1.78
11	1.87	1.58	1.58	1.85	1.79	1.59	1.76
12	1.76	1.65	1.66	1.99	1.92	1.65	1.83
13	1.46	1.34	1.35	1.48	1.46	1.35	1.41
14	1.52	1.54	1.53	1.57	1.65	1.54	1.61
15	2.52	2.26	2.33	2.61	2.53	2.29	2.45
16	1.36	1.22	1.25	1.38	1.34	1.26	1.33
17	0.39	0.43	0.43	0.26	0.31	0.36	0.31
18	0.25	0.40	0.40	0.23	0.28	0.34	0.28
19	1.00	0.90	0.85	0.97	0.96	0.85	0.88
20	2.82	2.07	2.01	2.94	2.72	2.29	2.86
21	2.51	1.84	1.82	2.50	2.37	1.98	2.32
22	3.86	3.77	3.83	4.00	3.96	3.76	3.90
23	4.01	3.81	3.87	4.30	4.21	3.84	4.14
24	3.24	2.53	2.60	3.09	2.97	2.55	2.89
25	3.27	2.11	2.07	3.24	2.94	2.28	2.80
26	3.14	2.91	2.91	3.46	3.35	3.08	3.29

27	4.25	2.52	2.31	4.20	3.90	2.76	3.65
28	4.01	2.46	2.26	4.08	3.75	2.71	3.50
29	3.27	2.27	2.22	3.08	2.91	2.47	3.01
30	2.14	1.97	1.95	2.37	2.32	2.10	2.32
31	3.38	3.37	3.42	3.53	3.50	3.38	3.44
32	3.30	3.55	3.58	3.79	3.74	3.59	3.70
33	3.23	3.51	3.54	3.78	3.72	3.53	3.66
34	1.60	1.71	1.95	1.04	1.17	1.44	1.20
35	1.51	1.75	1.93	1.24	1.35	1.49	1.26
36	3.09	2.85	2.82	3.45	3.34	2.88	3.15
37	2.24	1.99	1.98	2.24	2.20	1.91	2.04
38	1.90	2.03	2.07	2.05	2.07	1.93	1.93
39	1.84	2.09	2.13	2.13	2.15	1.99	2.00
40	3.43	3.69	3.63	4.30	4.20	3.66	3.97
41	2.24	1.70	1.72	1.81	1.80	1.61	1.65
42	2.15	2.26	2.29	2.41	2.42	2.12	2.18
43	0.81	1.05	1.05	1.17	1.14	1.05	1.11
44	0.53	0.72	0.69	0.67	0.70	0.71	0.68
45	0.62	0.55	0.54	0.45	0.49	0.51	0.45
46	0.98	0.62	0.61	0.61	0.62	0.63	0.63
47	0.76	0.63	0.64	0.74	0.71	0.68	0.69
48	0.64	0.71	0.70	0.62	0.65	0.69	0.64
49	0.67	0.70	0.69	0.63	0.65	0.68	0.64
50	0.00	0.00	0.00	0.00	0.00	0.00	0.00
51	0.00	0.01	0.01	0.01	0.01	0.01	0.01
52	0.00	0.01	0.01	0.01	0.01	0.01	0.01
53	0.00	0.00	0.00	0.00	0.00	0.00	0.00
54	0.00	0.02	0.02	0.03	0.03	0.02	0.03
55	2.70	1.83	1.91	2.25	2.14	1.79	2.04

56	3.60	2.82	2.88	3.13	3.05	2.98	2.98
57	2.64	2.02	2.18	2.75	2.54	1.80	2.17
58	1.24	1.10	1.13	1.04	1.05	1.05	1.03
59	0.93	0.68	0.71	0.94	0.87	0.70	0.79
60	0.89	0.79	0.80	0.83	0.84	0.78	0.80
61	1.52	1.56	1.60	2.14	1.99	1.54	1.87
62	3.03	2.73	2.76	3.17	3.06	2.66	2.90
63	4.25	3.67	3.70	4.00	3.92	3.55	3.74
64	1.60	1.53	1.55	1.50	1.63	1.50	1.60
65	1.53	0.82	0.87	0.80	0.81	0.79	0.80
66	0.00	0.00	0.00	0.00	0.00	0.00	0.00

Table S10. Comparison of experimental and COSMO-DFT/GTO-CP(PPP) calculated $|\Delta E_Q|$ values for the investigated data set of Fe complexes (values are given in mms^{-1})

complex	exptl.	RPBE	OLYP	B3LYP	B3LYP*	TPSS	TPSSh
1	0.34	0.55	0.54	0.33	0.39	0.50	0.40
2	0.77	1.12	1.12	0.70	0.98	1.02	0.83
3	0.21	0.05	0.05	0.09	0.06	0.02	0.08
4	1.84	1.76	1.77	1.60	1.64	1.69	1.64
5	1.72	1.86	1.89	2.08	2.03	1.86	1.97
6	2.75	2.84	2.86	2.99	2.98	2.82	2.90
7	2.86	2.62	2.64	3.43	3.20	2.68	3.02
8	2.38	2.44	2.44	3.28	3.08	2.50	2.85
9	1.88	1.73	1.73	1.95	1.91	1.74	1.83
10	1.82	1.77	1.76	2.02	1.96	1.79	1.89
11	1.87	1.77	1.76	2.04	1.98	1.80	1.91
12	1.76	1.73	1.73	2.05	1.98	1.74	1.89
13	1.46	1.41	1.41	1.55	1.52	1.41	1.47
14	1.52	1.50	1.50	1.61	1.59	1.50	1.54

15	2.52	2.08	2.16	2.42	2.34	2.13	2.27
16	1.36	1.10	1.13	1.24	1.21	1.13	1.19
17	0.39	0.49	0.48	0.31	0.36	0.43	0.36
18	0.25	0.38	0.38	0.23	0.27	0.34	0.27
19	1.00	0.96	0.96	0.95	0.95	0.93	0.92
20	2.82	2.63	2.56	3.38	3.25	2.79	3.16
21	2.51	3.09	3.00	3.46	3.57	3.21	3.56
22	3.86	3.64	3.67	3.83	3.79	3.64	3.74
23	4.01	3.61	3.64	4.07	3.99	3.66	3.92
24	3.24	2.69	2.75	3.24	3.12	2.73	3.04
25	3.27	2.74	2.67	3.63	3.45	2.93	3.36
26	3.14	3.28	3.23	3.87	3.78	3.42	3.68
27	4.25	3.15	2.94	4.68	4.52	3.45	4.28
28	4.01	2.82	2.61	4.21	4.11	3.27	3.99
29	3.27	2.74	2.70	3.41	3.29	2.87	3.21
30	2.14	2.97	2.98	3.08	3.09	2.99	3.04
31	3.38	3.59	3.61	3.74	3.72	3.60	3.66
32	3.30	3.57	3.56	3.74	3.72	3.58	3.65
33	3.23	3.53	3.52	3.73	3.70	3.54	3.63
34	1.60	1.00	1.81	0.40	0.49	0.73	0.55
35	1.51	1.78	2.04	1.21	1.33	1.45	1.26
36	3.09	2.94	2.93	3.52	3.41	2.95	3.21
37	2.24	2.06	2.07	2.29	2.25	1.97	2.10
38	1.90	2.09	2.12	2.10	2.12	1.96	1.97
39	1.84	2.17	2.20	2.19	2.21	2.03	2.05
40	3.43	3.68	3.69	4.22	4.12	3.70	3.96
41	2.24	2.10	2.13	2.20	2.21	1.97	2.00
42	2.15	2.22	2.26	2.33	2.34	2.06	2.09
43	0.81	0.71	0.71	0.81	0.79	0.69	0.74

44	0.53	0.72	0.71	0.66	0.68	0.70	0.66
45	0.62	0.52	0.52	0.43	0.46	0.48	0.42
46	0.98	0.94	0.93	0.88	0.90	0.93	0.91
47	0.76	0.52	0.52	0.62	0.58	0.52	0.58
48	0.64	0.71	0.70	0.61	0.64	0.69	0.63
49	0.67	0.73	0.72	0.65	0.68	0.72	0.67
50	0.00	0.03	0.03	0.03	0.04	0.04	0.05
51	0.00	0.01	0.01	0.00	0.01	0.00	0.01
52	0.00	0.00	0.01	0.01	0.01	0.00	0.00
53	0.00	0.00	0.00	0.00	0.00	0.00	0.00
54	0.00	0.01	0.01	0.01	0.01	0.01	0.01
55	2.70	2.32	2.42	2.84	2.71	2.28	2.58
56	3.60	3.04	3.12	3.34	3.27	2.97	3.17
57	2.64	2.08	2.20	2.84	2.62	2.00	2.44
58	1.24	0.97	0.97	0.98	0.99	0.97	0.98
59	0.93	0.56	0.55	0.93	0.87	0.59	0.77
60	0.89	0.88	0.93	0.95	0.93	0.85	0.91
61	1.52	1.71	1.76	2.22	2.07	1.70	1.95
62	3.03	2.82	2.86	3.27	3.15	2.77	3.01
63	4.25	3.88	3.89	4.21	4.13	3.76	3.96
64	1.60	1.73	1.77	1.91	1.84	1.65	1.73
65	1.53	1.18	1.23	1.25	1.25	1.12	1.18
66	0.00	0.01	0.01	0.01	0.01	0.01	0.01

Table S11. Comparison of experimental and COSMO-DFT/STO-TZP calculated $|\Delta E_Q|$ values for the investigated data set of Fe complexes (values are given in mms^{-1})

complex	exptl.	RPBE	OLYP	B3LYP	B3LYP*	TPSS	TPSSh
1	0.34	0.51	0.52	0.31	0.37	0.49	0.40
2	0.77	1.15	1.12	0.75	0.84	1.03	0.84
3	0.21	0.02	0.02	0.15	0.12	0.06	0.12
4	1.84	1.81	1.80	1.61	1.66	1.71	1.64
5	1.72	1.76	1.80	1.95	1.91	1.74	1.84
6	2.75	2.67	2.68	2.80	2.79	2.64	2.70
7	2.86	2.54	2.56	3.32	3.11	2.62	2.94
8	2.38	2.47	2.50	3.40	3.20	2.54	2.99
9	1.88	1.70	1.71	1.99	1.94	1.73	1.88
10	1.82	1.75	1.76	2.02	1.96	1.77	1.88
11	1.87	1.75	1.75	2.03	1.96	1.77	1.89
12	1.76	1.75	1.76	2.09	2.02	1.75	1.93
13	1.46	1.40	1.41	1.55	1.53	1.41	1.47
14	1.52	1.46	1.45	1.60	1.57	1.46	1.52
15	2.52	2.23	2.30	2.57	2.49	2.25	2.40
16	1.36	1.15	1.18	1.31	1.27	1.20	1.26
17	0.39	0.46	0.46	0.28	0.33	0.39	0.33
18	0.25	0.36	0.36	0.19	0.24	0.31	0.25
19	1.00	0.86	0.86	0.89	0.90	0.87	0.88
20	2.82	2.81	2.77	3.57	3.41	2.96	3.33
21	2.51	3.22	3.18	3.62	3.60	3.35	3.51
22	3.86	3.75	3.80	3.97	3.93	3.74	3.87
23	4.01	3.57	3.58	4.22	4.14	3.68	3.95
24	3.24	2.72	2.79	3.32	3.19	2.75	3.11
25	3.27	2.97	2.96	3.75	3.61	3.11	3.49
26	3.14	3.53	3.53	4.06	3.97	3.69	3.89

27	4.25	3.27	3.01	4.75	4.59	3.61	4.42
28	4.01	2.90	2.66	4.30	4.22	3.32	4.11
29	3.27	2.90	2.87	3.57	3.45	3.02	3.36
30	2.14	3.62	3.68	3.18	3.22	3.80	3.26
31	3.38	3.69	3.72	3.87	3.84	3.69	3.77
32	3.30	3.48	3.51	3.72	3.68	3.53	3.63
33	3.23	3.45	3.48	3.95	3.89	3.45	3.83
34	1.60	1.71	1.96	1.07	1.17	1.42	1.21
35	1.51	1.82	2.04	1.33	1.45	1.55	1.32
36	3.09	2.94	2.91	3.52	3.41	2.95	3.20
37	2.24	2.04	2.03	2.30	2.25	1.96	2.09
38	1.90	2.07	2.11	2.10	2.12	1.98	1.98
39	1.84	2.16	2.20	2.21	2.23	2.06	2.07
40	3.43	3.63	3.63	4.22	4.12	3.69	3.99
41	2.24	2.12	2.16	2.23	2.24	2.01	2.04
42	2.15	2.21	2.25	2.37	2.37	2.08	2.14
43	0.81	0.70	0.70	0.81	0.79	0.70	0.74
44	0.53	0.69	0.66	0.63	0.65	0.67	0.64
45	0.62	0.54	0.53	0.43	0.47	0.49	0.43
46	0.98	0.90	0.89	0.86	0.88	0.91	0.89
47	0.76	0.51	0.52	0.62	0.68	0.51	0.58
48	0.64	0.66	0.64	0.56	0.59	0.64	0.58
49	0.67	0.68	0.66	0.60	0.63	0.66	0.62
50	0.00	0.00	0.00	0.00	0.00	0.00	0.00
51	0.00	0.01	0.01	0.01	0.01	0.01	0.01
52	0.00	0.01	0.01	0.00	0.00	0.00	0.00
53	0.00	0.01	0.00	0.00	0.00	0.00	0.00
54	0.00	0.00	0.00	0.00	0.00	0.00	0.00
55	2.70	2.36	2.48	2.92	2.78	2.31	2.63

56	3.60	3.30	3.33	3.65	3.56	3.22	3.45
57	2.64	1.94	2.10	2.71	2.49	1.82	2.26
58	1.24	1.08	1.11	1.05	1.06	1.04	1.03
59	0.93	0.77	0.79	1.08	1.01	0.80	0.91
60	0.89	0.93	0.97	0.98	0.97	0.90	0.94
61	1.52	1.52	1.57	2.11	1.95	1.50	1.83
62	3.03	2.69	2.73	3.16	3.04	2.61	2.87
63	4.25	3.93	3.96	4.26	4.18	3.80	4.00
64	1.60	1.78	1.82	1.89	1.82	1.70	1.76
65	1.53	1.38	1.42	1.38	1.39	1.34	1.35
66	0.00	0.00	0.00	0.00	0.00	0.00	0.00

Table S12. Comparison of experimental and COSMO-TPSSh $|\Delta E_Q|$ values for selected Fe complexes computed with the GTO-CP(PPP) basis set at different geometries (values are given in mms^{-1})

Complex	Exp.	BP86 geometry	COSMO-TPSSh geometry
8	2.38	2.85	2.86
21	2.51	3.56	3.62
26	3.14	3.68	3.73
30	2.14	3.04	3.23
34	1.60	0.55	0.59
40	3.43	3.96	3.96

Table S13. DFT- and COSMO-DFT calculated values of the asymmetry parameter (η) obtained with the GTO-CP(PPP) basis set

complex	RPBE	B3LYP	COSMO-RPBE	COSMO-B3LYP
1	0.03	0.23	0.05	0.18
2	0.98	0.90	0.87	0.58
3	0.25	0.21	0.22	0.20
4	0.02	0.02	0.02	0.03
5	0.00	0.00	0.01	0.01
6	0.00	0.00	0.00	0.00
7	0.84	0.70	0.89	0.77
8	0.01	0.01	0.01	0.01
9	0.08	0.07	0.09	0.08
10	0.36	0.28	0.52	0.45
11	0.32	0.26	0.48	0.42
12	0.55	0.57	0.51	0.54
13	0.23	0.14	0.24	0.12
14	0.01	0.01	0.02	0.02
15	0.01	0.01	0.01	0.01
16	0.01	0.01	0.01	0.01
17	0.01	0.02	0.02	0.01
18	0.01	0.02	0.03	0.01
19	0.00	0.00	0.00	0.00
20	0.23	0.48	0.09	0.41
21	0.97	0.31	0.51	0.95
22	0.03	0.05	0.03	0.05
23	0.94	0.20	0.89	0.19
24	0.36	0.36	0.47	0.47
25	0.30	0.56	0.26	0.90
26	0.00	0.00	0.00	0.00

27	0.17	0.04	0.21	0.04
28	0.24	0.05	0.14	0.05
29	0.22	0.48	0.19	0.37
30	0.94	0.42	0.20	0.06
31	0.10	0.08	0.70	0.57
32	0.00	0.00	0.00	0.00
33	0.00	0.00	0.00	0.00
34	0.04	0.01	0.12	0.02
35	0.06	0.03	0.08	0.67
36	0.29	0.36	0.18	0.22
37	0.31	0.40	0.37	0.47
38	0.05	0.08	0.06	0.09
39	0.06	0.08	0.06	0.10
40	0.00	0.00	0.00	0.00
41	0.09	0.08	0.34	0.35
42	0.60	0.49	0.57	0.44
43	0.80	0.69	0.26	0.36
44	0.30	0.08	0.47	0.23
45	0.00	0.00	0.00	0.00
46	0.26	0.40	0.97	0.85
47	0.33	0.16	0.48	0.38
48	0.01	0.01	0.03	0.02
49	0.04	0.06	0.02	0.05
50	0.40	0.46	0.05	0.23
51	0.38	0.25	0.76	0.10
52	0.18	0.69	0.17	0.91
53	0.00	0.02	0.58	0.50
54	0.30	0.29	0.19	0.18
55	0.11	0.10	0.10	0.10

56	0.35	0.39	0.39	0.43
57	0.08	0.02	0.23	0.02
58	0.16	0.24	0.15	0.23
59	0.06	0.01	0.08	0.04
60	0.84	0.88	0.73	0.77
61	0.06	0.07	0.06	0.04
62	0.21	0.12	0.21	0.10
63	0.80	0.74	0.79	0.73
64	0.78	0.61	0.45	0.66
65	0.69	0.54	0.27	0.21
66	0.52	0.74	0.48	0.79

Table S14. DFT- and COSMO-DFT calculated values of the asymmetry parameter (η) obtained with the STO-TZP basis set

complex	RPBE	B3LYP	COSMO-RPBE	COSMO-B3LYP
1	0.11	0.45	0.14	0.36
2	0.98	0.92	0.88	0.58
3	0.43	0.07	0.55	0.06
4	0.01	0.01	0.02	0.01
5	0.00	0.00	0.01	0.01
6	0.00	0.00	0.01	0.01
7	0.83	0.68	0.88	0.77
8	0.01	0.00	0.01	0.00
9	0.08	0.08	0.09	0.08
10	0.28	0.23	0.48	0.43
11	0.26	0.21	0.44	0.40
12	0.60	0.60	0.56	0.56
13	0.18	0.11	0.18	0.11
14	0.01	0.01	0.02	0.02

15	0.01	0.01	0.01	0.01
16	0.01	0.01	0.01	0.01
17	0.00	0.00	0.00	0.01
18	0.00	0.00	0.01	0.03
19	0.00	0.00	0.04	0.06
<hr/>				
20	0.25	0.15	0.33	0.06
21	0.94	0.29	0.45	0.76
22	0.30	0.07	0.27	0.07
23	0.00	0.00	0.37	0.05
24	0.42	0.40	0.53	0.53
25	0.27	0.47	0.28	0.55
26	0.00	0.00	0.02	0.02
27	0.16	0.04	0.19	0.05
28	0.22	0.02	0.10	0.05
29	0.21	0.13	0.50	0.27
30	0.80	0.45	0.55	0.38
31	0.10	0.08	0.70	0.56
32	0.02	0.01	0.02	0.01
33	0.02	0.01	0.02	0.06
<hr/>				
34	0.08	0.64	0.12	0.68
35	0.09	0.66	0.16	0.72
<hr/>				
36	0.27	0.35	0.16	0.20
37	0.24	0.34	0.28	0.39
38	0.00	0.00	0.01	0.01
39	0.00	0.00	0.03	0.03
40	0.00	0.00	0.01	0.01
41	0.08	0.06	0.35	0.38
42	0.59	0.51	0.58	0.47
<hr/>				
43	0.78	0.67	0.34	0.46

44	0.32	0.08	0.50	0.25
45	0.00	0.00	0.02	0.02
46	0.28	0.38	0.88	0.80
47	0.24	0.18	0.44	0.37
48	0.02	0.03	0.04	0.05
49	0.03	0.05	0.02	0.04
50	0.92	0.90	0.90	0.43
51	0.80	0.82	0.61	0.85
52	0.13	0.30	0.00	0.00
53	0.02	0.01	0.42	0.67
54	0.30	0.24	0.01	0.13
<hr/>				
55	0.11	0.10	0.10	0.09
56	0.36	0.39	0.42	0.45
57	0.16	0.03	0.29	0.01
<hr/>				
58	0.17	0.24	0.16	0.23
59	0.07	0.01	0.10	0.05
60	1.00	0.99	0.68	0.69
61	0.05	0.10	0.03	0.06
62	0.24	0.16	0.23	0.13
<hr/>				
63	0.80	0.76	0.81	0.75
64	0.96	0.82	0.28	0.39
<hr/>				
65	0.44	0.37	0.18	0.14
66	0.12	0.20	0.00	0.00

Table S15. DFT-calculated ΔE_Q values obtained for the *cis-trans* isomers of FeA_4B_2 and for the FeA_5B low-spin, model compounds (values are given in mms^{-1})

complex	<i>trans</i> - FeA_4B_2	<i>cis</i> - FeA_4B_2	FeA_5B
$\text{Fe}(\text{CN})_2(\text{CO})_4$	-1.08	+0.48	-0.65
$\text{Fe}(\text{CN})_4(\text{CO})_2$	+0.71	-0.33	+0.37
$\text{Fe}(\text{CN})_2(\text{NCS})_4$	-1.38	+0.69	-0.63
$\text{Fe}(\text{CN})_4(\text{NCS})_2$	+1.52	-0.81	+0.81
$\text{Fe}(\text{CN})_2(\text{PMe}_3)_4$	-1.23	+0.74	-0.69
$\text{Fe}(\text{CN})_4(\text{PMe}_3)_2$	+0.81	-0.53	+0.40
$\text{Fe}(\text{CO})_2(\text{CH}_3\text{CN})_4$	-0.51	+0.23	-0.25
$\text{Fe}(\text{CO})_4(\text{CH}_3\text{CN})_2$	+0.50	-0.26	+0.20

In all cases, the COSMO-TPSSh/STO-TZP method was applied.

Table S16. Comparison of the experimental and DFT-calculated signs of V_{zz}

complex	exptl. ^a	COSMO-TPSSh
1		-
2		-
3		+
4		+
5	+	+
6		+
7		-
8	+	+
9		+
10		+
11		+
12		+
13	-	-
14		+

15	+	+
16		+
17		-
18		-
19		-
<hr/>		
20		-
21		+
22		-
23	-	-
24	-	-
25	-	-
26		+
27	+	+
28	+	+
29		-
30		+
31 ^b	+/-	+/-
32		+
33		+
<hr/>		
34	+	+
35	+	+
<hr/>		
36		-
37		+
38		+
39		+
40	-	-
41	-	-
42		-
<hr/>		

43		–
44		–
45		–
46		–
47		+
48		+
49		+
50		
51		+
52		
53		
54		
<hr/>		
55		+
56	+	+
57		+
<hr/>		
58		+
59	+	+
60	–	–
61		+
62		+
<hr/>		
63	+	+
64	–	–
<hr/>		
65		+
66		

^aThe experimental sign of V_{zz} is given, if it was determined by applied-field Mössbauer spectroscopy. ^bThe negative and positive signs correspond to the orbital singlet and doublet state, respectively.

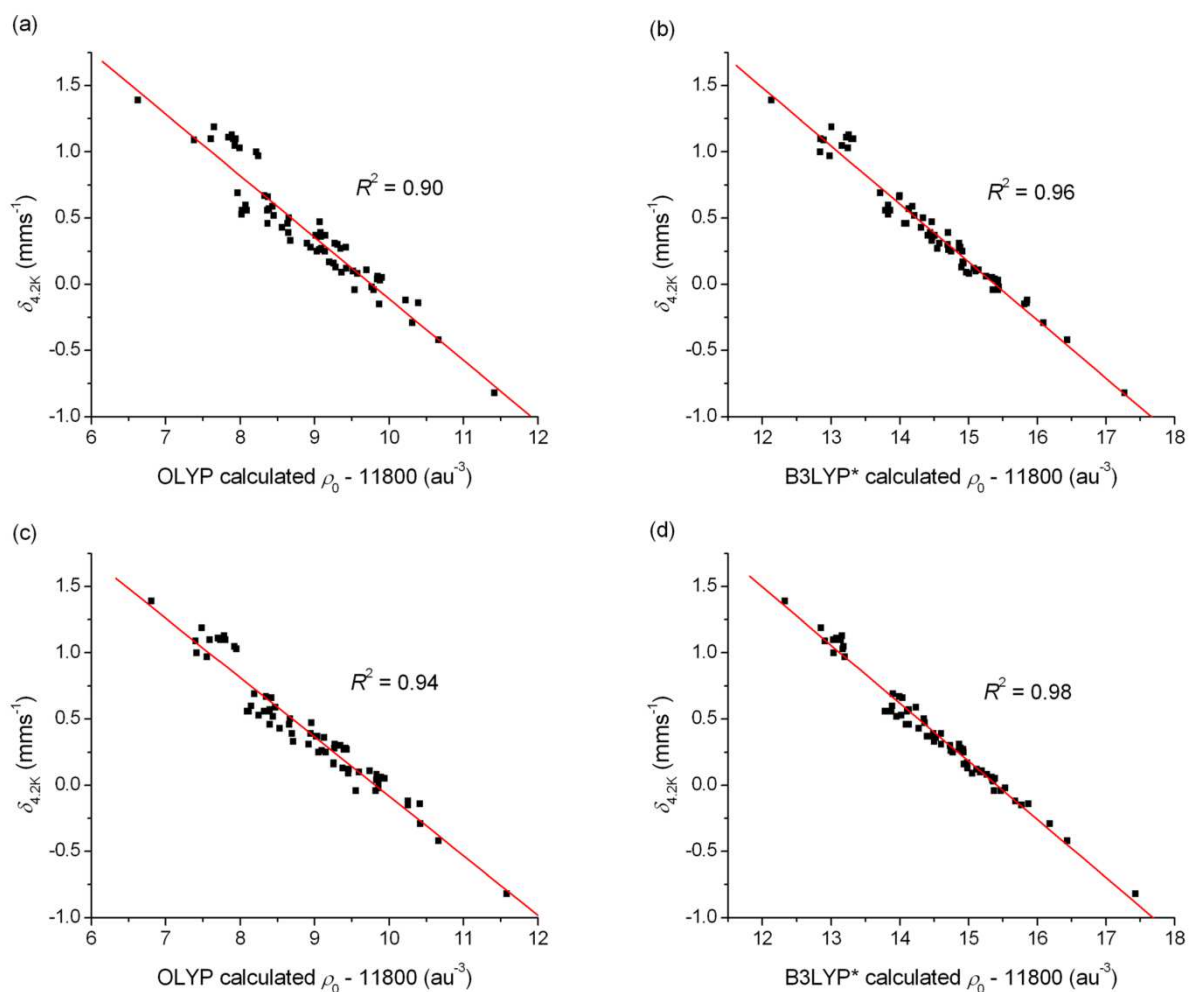


Figure S2. DFT linear correlations between the (a) OLYP, (b) B3LYP*, (c) COSMO-OLYP, (d) COSMO-B3LYP* (in combination with the GTO-CP(PPP) basis set) calculated electron density (ρ_0) at the ^{57}Fe nucleus and the corrected experimental isomer shift ($\delta_{4,2K}$). Correlations for all other applied DFT methods are shown in the SI.

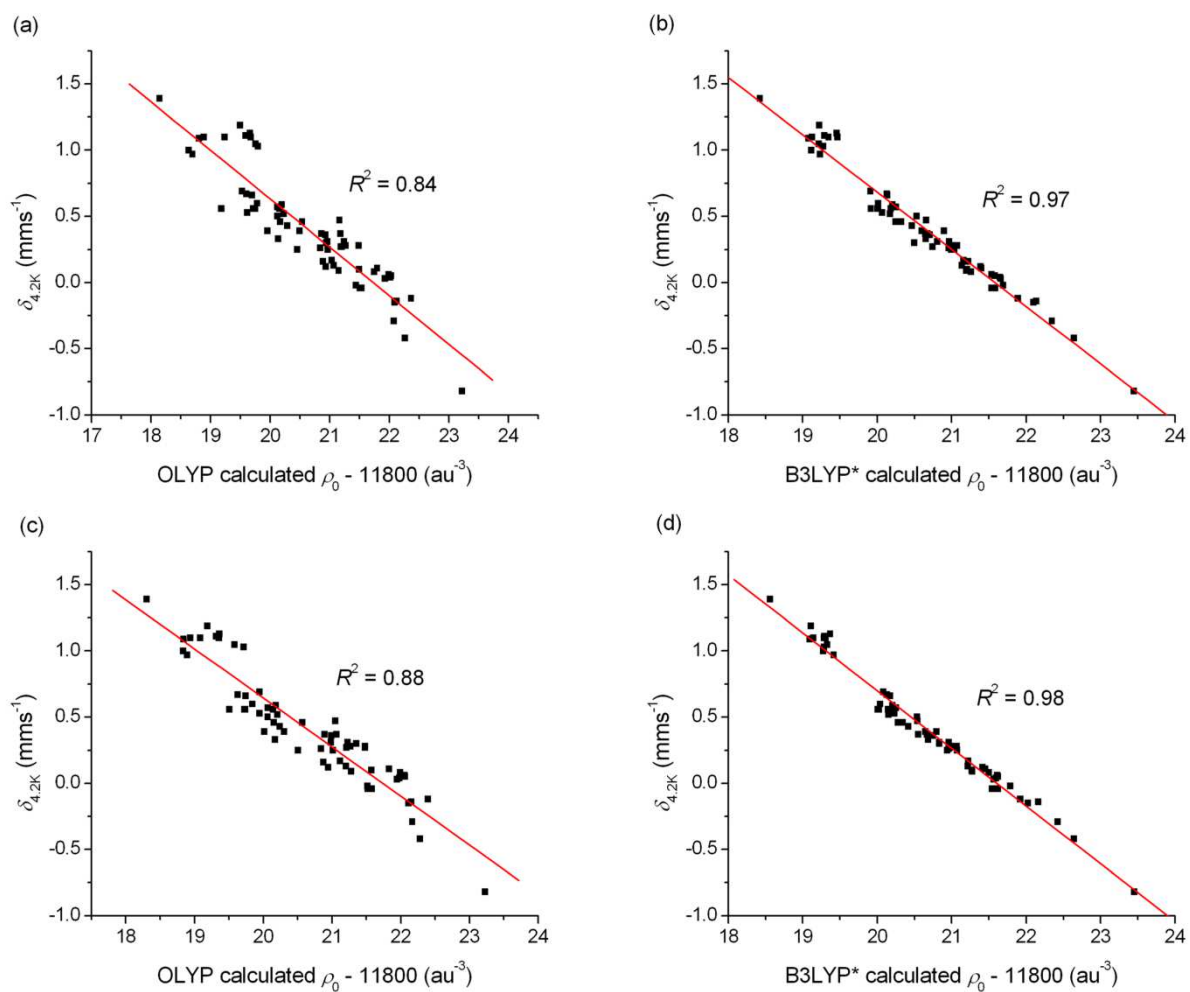


Figure S3. DFT linear correlations between the (a) OLYP, (b) B3LYP*, (c) COSMO-OLYP, (d) COSMO-B3LYP* (in combination with the STO-TZP basis set) calculated electron density (ρ_0) at the ^{57}Fe nucleus and the corrected experimental isomer shift ($\delta_{4,2K}$). Correlations for all other applied DFT methods are shown in the SI.

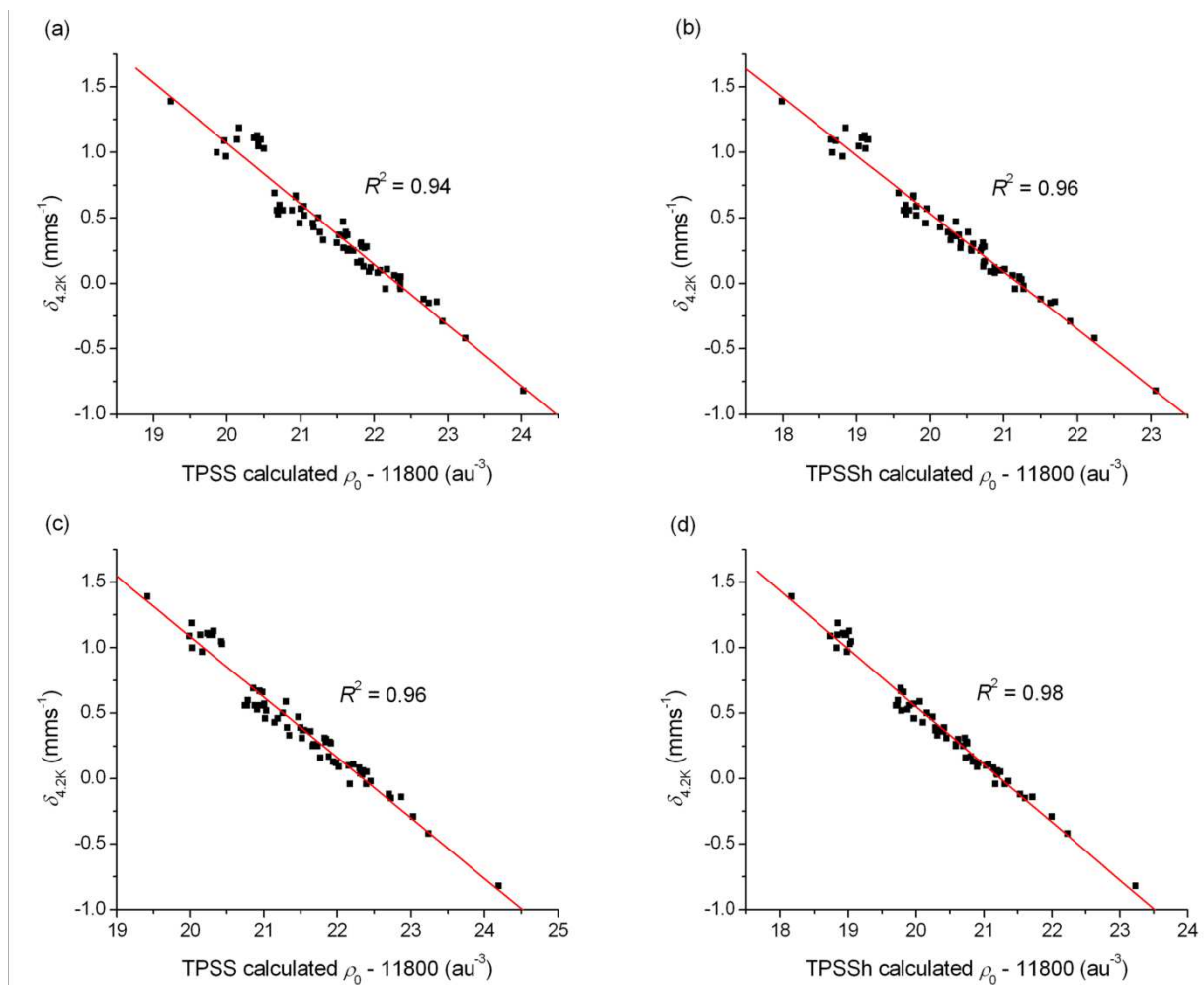


Figure S4. DFT linear correlations between the (a) TPSS, (b) TPSSh, (c) COSMO-TPSS, (d) COSMO-TPSSh (in combination with the GTO-CP(PPP) basis set) calculated electron density (ρ_0) at the ^{57}Fe nucleus and the corrected experimental isomer shift ($\delta_{4,2K}$). Correlations for all other applied DFT methods are shown in the SI.

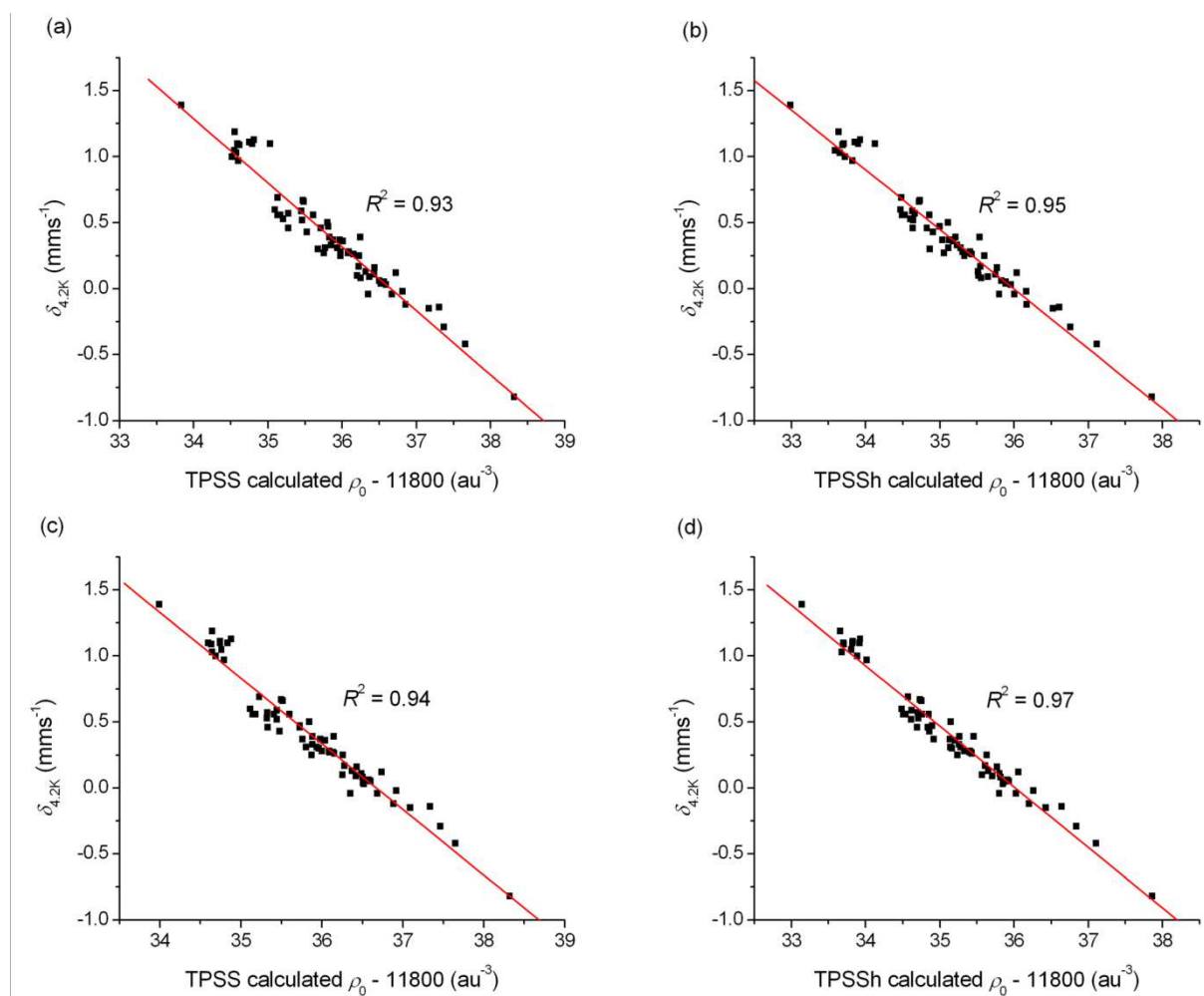


Figure S5. DFT linear correlations between the (a) TPSS, (b) TPSSh, (c) COSMO-TPSS, (d) COSMO-TPSSh (in combination with the STO-TZP basis set) calculated electron density (ρ_0) at the ⁵⁷Fe nucleus and the corrected experimental isomer shift ($\delta_{4,2K}$). Correlations for all other applied DFT methods are shown in the SI.

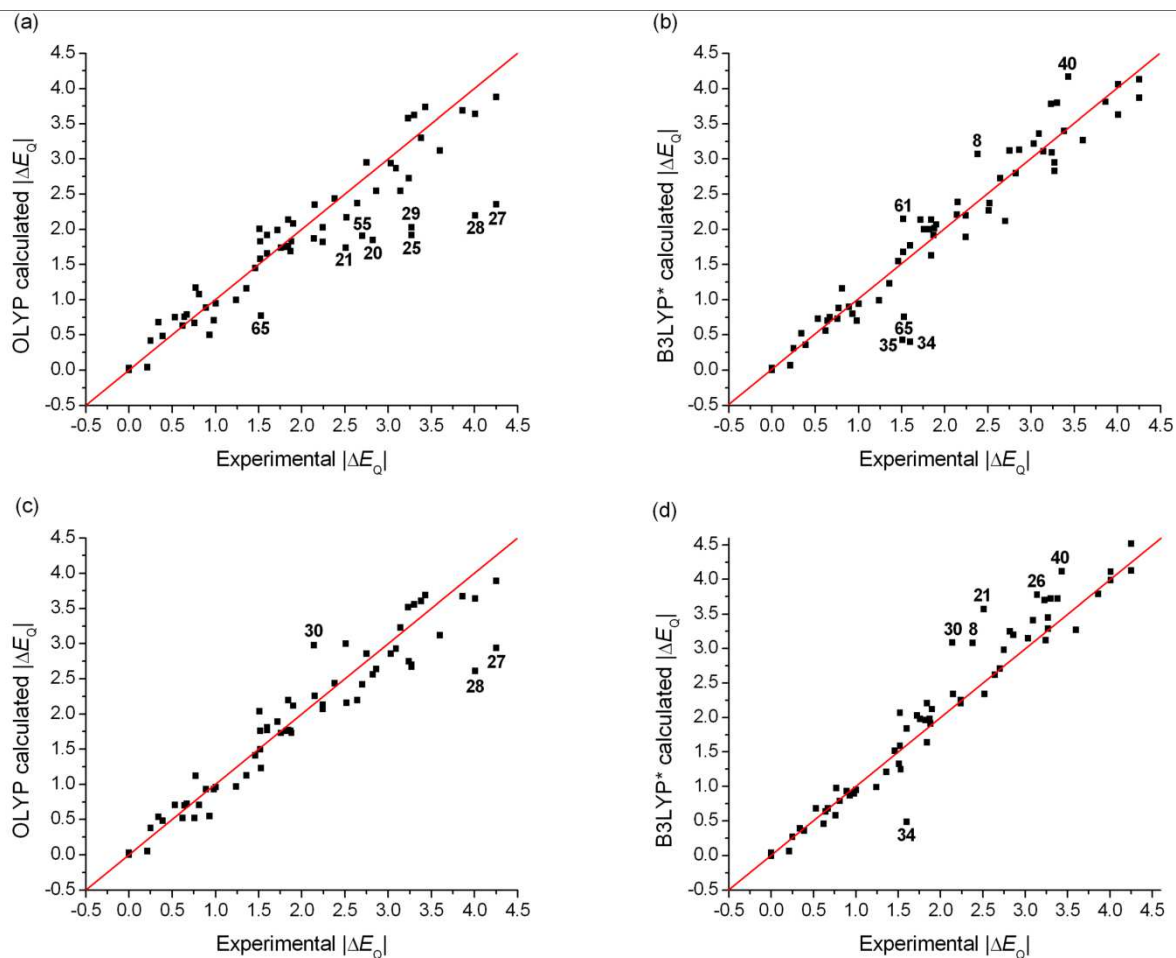


Figure S6. Comparison of experimental and (a) OLYP, (b) B3LYP*, (c) COSMO-OLYP, (d) COSMO-B3LYP* (in combination with the GTO-CP(PPP) basis set) calculated quadrupole splittings (ΔE_Q). The red line connects the $\Delta E_Q(\text{exp.}) = \Delta E_Q(\text{calc.})$ points.

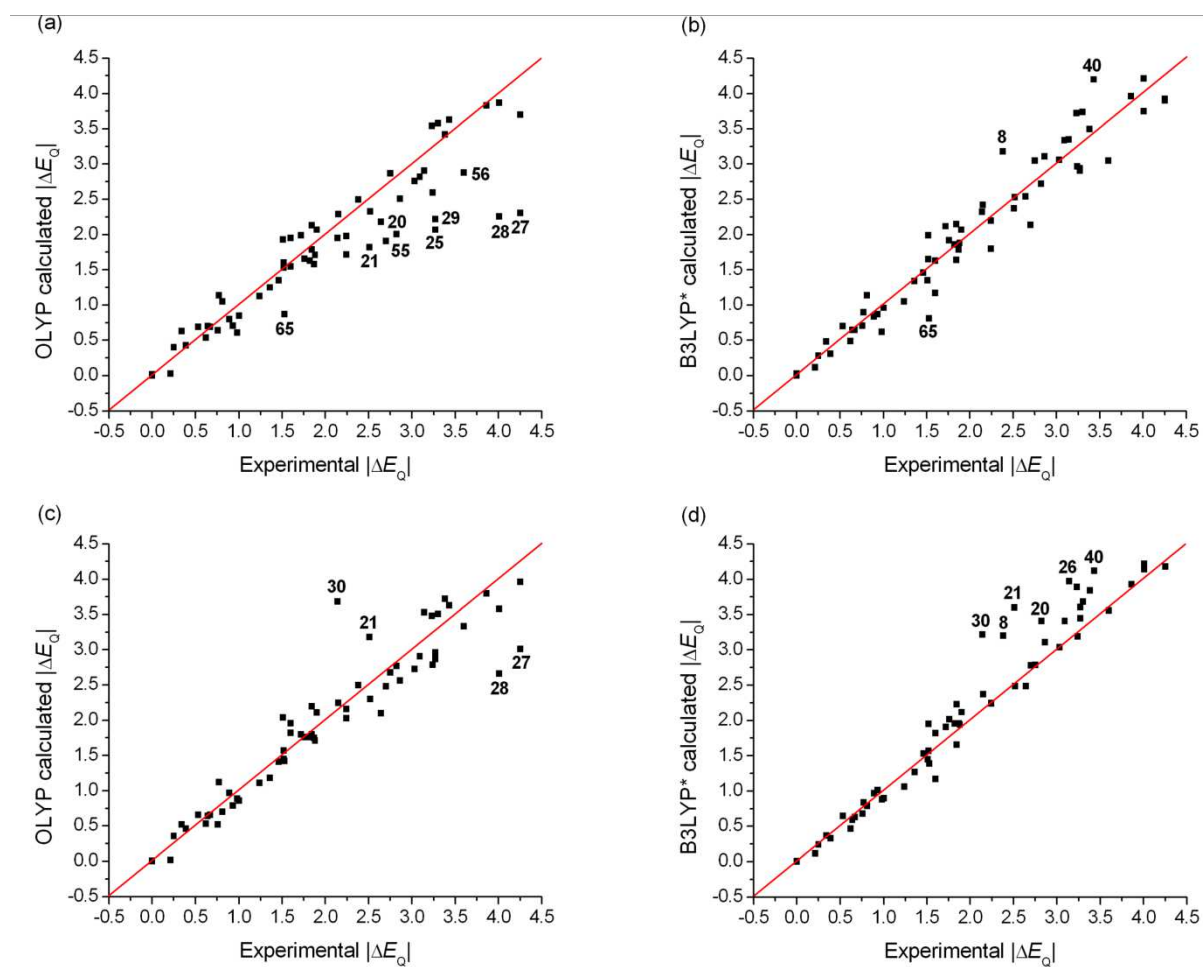


Figure S7. Comparison of experimental and (a) OLYP, (b) B3LYP*, (c) COSMO-OLYP, (d) COSMO-B3LYP* (in combination with the STO-TZP basis set) calculated quadrupole splittings (ΔE_Q). The red line connects the $\Delta E_Q(\text{exp.}) = \Delta E_Q(\text{calc.})$ points.

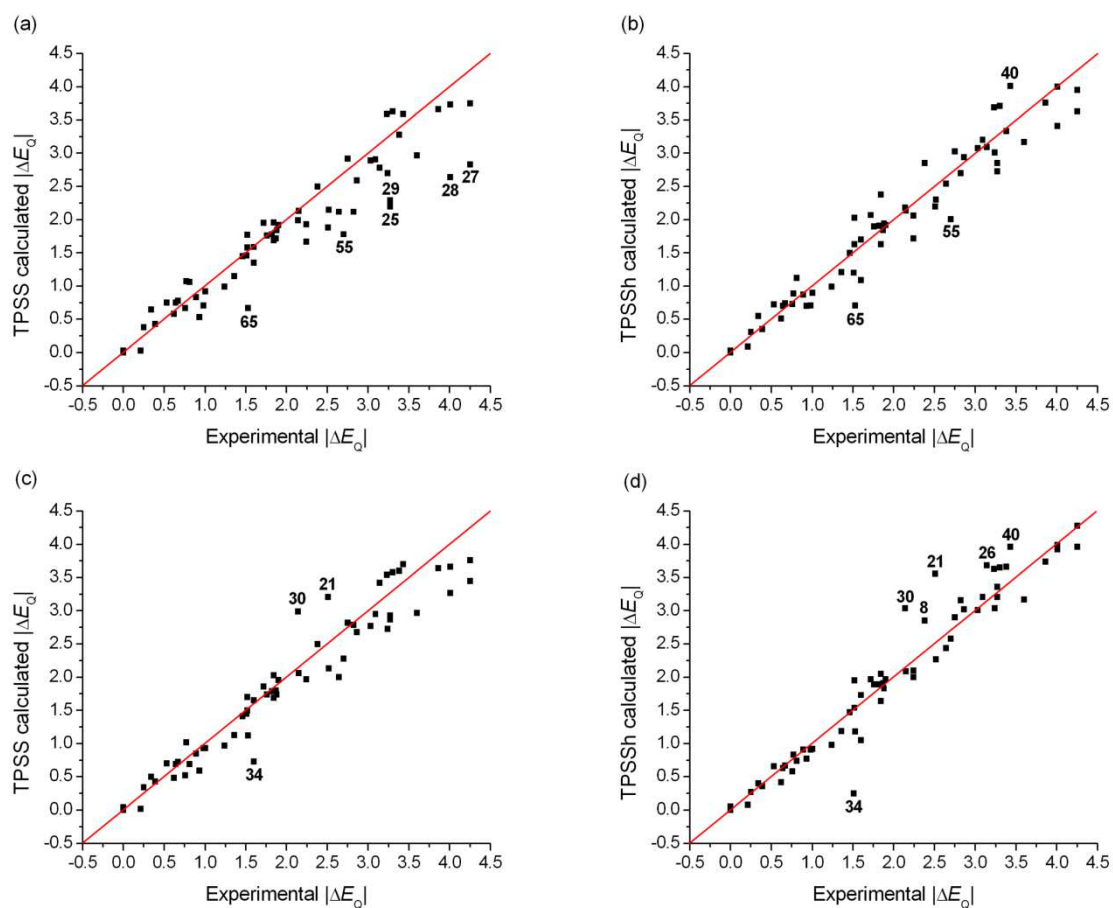


Figure S8. Comparison of experimental and (a) TPSS, (b) TPSSh, (c) COSMO-TPSS, (d) COSMO-TPSSh (in combination with the GTO-CP(PPP) basis set) calculated quadrupole splittings (ΔE_Q). The red line connects the $\Delta E_Q(\text{exp.}) = \Delta E_Q(\text{calc.})$ points.

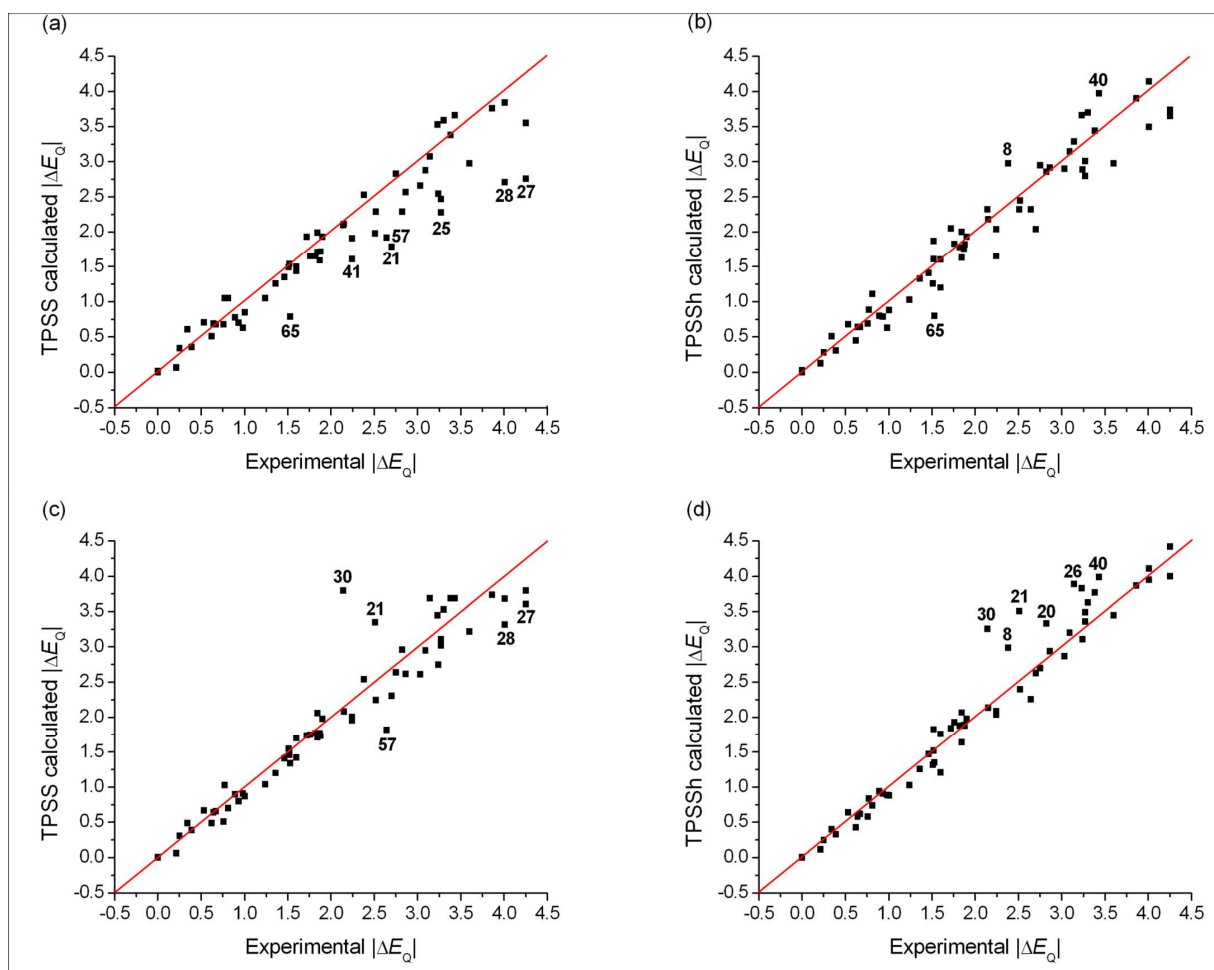


Figure S9. Comparison of experimental and (a) TPSS, (b) TPSSh, (c) COSMO-TPSS, (d) COSMO-TPSSh (in combination with the STO-TZP basis set) calculated quadrupole splittings (ΔE_Q). The red line connects the $\Delta E_Q(\text{exp.}) = \Delta E_Q(\text{calc.})$ points.